scientific reports

Check for updates

OPEN

Development of an original PAm@P hydrogel for high-performance cationic dye removal from wastewater

AbdElAziz A. Nayl[1]✉, Wael A. Arafa[1], Ismail M. Ahmed[1], Ahmed Hamad Alanazi[1], Meshari D. Alanazi[2], Aya G. Mostafa[3], Magda Aly Akl[3], Stefan Bräse[4]✉ & Ahmed I. Abd-Elhamid[5]

In this study, an original and simple method was employed to modify polyacrylamide (PAm) with sodium phosphate (Na_3PO_4), yielding a sodium phosphate-modified polyacrylamide hydrogel (PAm@P) with promising swelling and adsorption properties compared to pristine, unmodified polyacrylamide. The PAm@P hydrogel was characterized using various advanced techniques to confirm successful modification of PAm and the formation of the PAm@P hydrogel. Swelling experiments demonstrated that phosphate modification significantly enhanced the swelling capacity of PAm@P hydrogel (%S = 7000 at t = 60 min and pH 9.5) compared to unmodified PAm. The adsorption performance of PAm@P was evaluated using methylene blue (MB) dye. The adsorption kinetics followed a pseudo-second-order model exhibiting the best fit with the highest value for the correlation factor (R^2) of 0.999, comparing with R^2 values obtained for the other investigated models (0.976, 0.976, 0.993, and 0.654 for Pseudo first order, Liquid film diffusion, and intra-particle diffusion (step1 and step 2) kinetic models, respectively. These results demonstrated that the investigated adsorption process may be explained as chemisorption is the dominant mechanism. Also, the Langmuir isotherm model illustrated the R^2 value (0.999) with a maximum monolayer adsorption capacity (q_{max}) of 746.26 mg g^{-1} for MB dye. While the R^2 values for the other investigated adsorption isotherm models were 0.254, 0.672, and 0.704 for Freundlich, Tempkin, and Flory-Higgins models, respectively. Also, the highest experimental adsorption capacity (q_{max} = 1490 mg g^{-1}) was obtained under the optimum adsorption conditions with an initial MB-dye concentration of 300 mg L^{-1}, PAm@P hydrogel dosage of 0.005 g, solution volume of 25 mL, pH 7, contact time of 120 min, and temperature of 25 °C. Furthermore, the PAm@P hydrogel exhibited selective adsorption and separation of the cationic dye MB in the presence of other dyes, such as Rhodamine B (RhB) and Azorubine (E122). The adsorption selectivity of the fabricated PAm@P hydrogel was quantitatively evaluated by calculating the selectivity factor (SF) where it was 2.31 for MB/Rhodamine B and 3.10 for MB/E122, confirming the preferential adsorption of MB-due over the other investigate dyes under identical experimental conditions. Moreover, the PAm@P hydrogel exhibited good regeneration and reusability performance over three consecutive adsorption–desorption cycles. The adsorption efficiency decreased gradually from 96.56% in the first cycle to 62.63% after the third cycle, indicating that approximately 64.9% of the initial adsorption efficiency was retained. Finally, the application of the prepared PAm@P hydrogel to real wastewater samples demonstrated its practical feasibility and highlighted its potential as an efficient adsorbent material for industrial wastewater treatment applications. This confirms that the investigated hydrogel is economical, promising, and can significantly reduce wastewater pollutants.

Keywords Polyacrylamide, Polyacrylamide@phosphate, Hydrogel, Adsorption, Swelling, Methylene blue, Wastewater treatment

[1]Department of Chemistry, College of Science, Jouf University, Sakaka 72341, Al Jouf, Saudi Arabia. [2]Department of Electrical Engineering, College of Engineering, Jouf University, Sakakah 72388, Saudi Arabia. [3]Chemistry Department of Chemistry, Faculty of Science, Mansoura University, Mansoura 35516, Egypt. [4]Institute of Biological and Chemical Systems – Functional Molecular Systems (IBCS-FMS), Kaiserstrasse 12, 76131 Karlsruhe, Germany. [5]Composites and Nanostructured Materials Research Department, Advanced Technology and New Materials Research Institute, City of Scientific Research and Technological Applications (SRTA-City), New Borg Al-Arab, Alexandria 21934, Egypt. ✉email: aanayel@ju.edu.sa; aanayl@yahoo.com; stefan.braese@kit.edu

During the last decades, global freshwater demand has increased dramatically due to unsustainable water resource management, population growth, and rising industrial activities[1]. Freshwater resources are considered essential for maintaining ecosystems and supporting human life[2]. Nowadays, various water bodies worldwide are increasingly polluted by the discharge of dye-containing wastewater and other contaminants into the surrounding environment. Different industrial effluents, particularly those containing synthetic dyes, represent a major environmental challenge and significantly hinder water restoration efforts[3,4]. One of the most serious consequences of modern industrial applications is the discharge of untreated industrial wastewater into aquatic systems, especially effluents containing colored dyes[5–7]. Over the past few decades, with the drastic augmentation in the production capacities of synthetic dyes, contamination of organic dyes after being discharged into water has become a major component of pollutants that has great harm to the environment[8,9]. Cationic dyes constitute the largest share of synthetic dyes that pose serious environmental threats to aquatic ecosystems and human health, rendering their removal extremely difficult[7,8]. MB dye is regarded as one of the most toxic and harmful cationic dyes with a complex aromatic structure that are used on a large scale in various industrial applications[10,11]. In addition to its potential hazard to human health, discharging wastewater containing (MB)-dye leads to serious damage to the ecological environment, where it is difficult to decompose in aqueous media[11–14]. Due to the recent increase in the industrial applications of (MB)-dye, removing it from colored wastewater to a risk-free level is becoming increasingly urgent and a hot topic, given the improper discharge of these wastes into the environment[15]. Among various industries, the textile and dyeing sectors are major contributors to dye-contaminated wastewater, as reported in the annual wastewater report[13]. The global annual production of synthetic dyes exceeding 8.0×10^7 tons of synthetic dyes[2], and about 1.0–10% of the dyes used during textile dyeing processes are lost and discharging into the environment and potentially disturbing aquatic organisms[15]. In Egypt, exceeding 10% of dyestuffs are lost also in industrial effluents. The contaminated textile effluents generally contain dye concentrations more than 10 mg L, depending on the dyeing processes and industrial sources. Furthermore, even dye concentrations below 1.0 mg L^{-1} are sufficient to impart visible color to receiving waters, adversely affecting photosynthetic activity, and other environmental concerns. Therefore, treatment and decontamination of such wastewater are essential to meet global water sustainability requirements[16]. To keep freshwater resources available for the growing population, developing advanced processes is becoming crucial for treating wastewater contaminated by these pollutants[13]. Recently, various technologies have been developed and used to treat wastewater from organic dyes, especially MB from wastewater, including membrane filtration, adsorption, biological degradation, coagulation, reverse osmosis, chemical reduction, chemical oxidation, advanced oxidation processes, electrochemical reduction, catalytic degradation, and flotation[5,6,10,12]. Among these, adsorption methods are regarded as the most promising and commonly used processes due to their ease of design, lower operating costs, adaptability, ease of recovering adsorbent materials, high efficiency, and eco-friendliness. They can completely decolorize dyes[5,6,10,17,18]. However, conventional adsorbents often suffer from limitations such as low capacity, poor selectivity, and limited reusability. Consequently, researchers have focused on developing advanced nanostructured materials with enhanced adsorption performance[12]. Nanomaterials offer high surface area and abundant active sites, making them highly effective for dye removal[6]. One of the most advanced nanomaterials that can be utilized to overcome many environmental issues is filled hydrophilic systems. Nanomaterial hydrogels represent a notable advancement in hydrogel-based nanomaterials[2]. Recently, due to the marvelous adsorption capabilities, the biocompatible and multifunctional of hydrogels materials, they have gained great scientific attention and considered as innovative materials[19]. Also, hydrogels materials have attracted considerable interest in the recent years among the numerous adsorbents due to their unique properties such as porous structures, high surface-to-volume ratios, higher adsorption capacities, biodegradability, biocompatibility, reusability, distinctive physical properties, and sensitivities to environmental stimuli where they have different ionic function groups, making selective removal of dissolved pollutants in wastewater, such as anionic and cationic dyes[19–22]. Recently, a novel hydrogel adsorbent, HG-cl-poly(MAA), was investigated to remove MB molecules from wastewater with maximum adsorption capacities of 284 mg g^{-1}[19]. Another green adsorbent (Stg-(AA-AAM) was designed to remove Malachite Green (MG) dye from aqueous media with q_{max} reached 18.36 mgg^{-1}[20]. The fabrication and studying the adsorption performance of carboxymethyl cellulose-based silica (CMC/AA/AAm/SiO_2) hydrogel nanocomposite was investigated to remove MB and MG dyes from aquatic media with q_{max} of 752.9 mg g^{-1} for MB and 906.3 mg g^{-1} for MG[21]. Xanthan gum/acrylic acid/acrylamide modified with graphene oxide (XG/AA/AAm and XG/AA/AAm/GO) hydrogels were synthesized as effective adsorbents for the removal of MB dye with q_{max} of 730.7 and 1008 mg g^{-1}, respectively[22]. The promising properties of hydrogels enable the selective removal of dissolved contaminants, including cationic and anionic dyes. Despite their advantages, hydrogels often suffer from weak mechanical strength and limited recyclability[9,22]. To overcome these limitations, the incorporation of inorganic components into polymer networks has been widely investigated[22]. Polymeric hydrogel materials like PAm have been investigated as promising materials for

environmental scientists due to their notable characteristics, such as environmentally friendly behavior, economic feasibility, and adsorption-regeneration, as well as their ability to endow hydrogels with mechanical strength[9,23]. PAm hydrogels are functionalized polymers with large number of amide groups, which are considered abundant active sites, making them capable of adsorbing dye molecules, metals, and organic compounds, etc., in addition to their unique chemical and molecular structures[23,24]. Recently, many studies in this area have focused on modifying PAm to improve its properties as an adsorbent material[25]. Chemical or physical routes are the more common methods for modifying PAm. Copolymerization and grafting arethemore common processes involved in the chemical modification route[26–29]. While H-bond and simple blinding PAm with other materials, depending on internal attraction forces, are investigated in the physical modification routes[30,31]. Consequently, many studies have been conducted to investigate and improve the adsorption performance and characteristics of hydrogel materials, as well as to reduce costs and simplify their preparation by incorporating polymer networks with inorganic metals via different routes[32]. Despite the wide application of PAm-based hydrogels in adsorption processes, there remains a clear limitation in achieving high selectivity and strong affinity toward cationic dyes using conventional PAm systems. Most reported PAm-based hydrogels lack sufficient functional groups that can provide strong electrostatic attractions and effectiveness adsorption active sites for efficient dye removal, which limits their efficiency and selectivity toward cationic dyes in aquatic media. Moreover, limited studies have explored phosphate-embedded polyacrylamide hydrogels for MB-dye adsorption. Therefore, there is still a need to enhance the chemical functionality of PAm-based hydrogels to improve their adsorption efficiency and selectivity. Hence, the present work aims to develop an efficient polyacrylamide@phosphate (PAm@P) hydrogel with enhanced adsorption capacity for MB removal from aqueous solutions. To the best of our knowledge, few and limited studies have explored phosphate-embedded PAm-based hydrogels for MB molecules adsorption from aqueous environments. Therefore, the aim of the current work is to investigate a novel modified PAm@P hydrogel with an increased adsorption performance to adsorb MB dye. The preparation of PAm employed radical polymerization route was investigated to yield bulk mass of hydrogel. Thereafter, the obtained bulk hydrogel breakdown using homogenizer to produce micro-size hydrogel. Then, the micro gel was modified with phosphate groups using trisodium phosphate. Due to the breaking process, the active sites will be greatly exposure to the outer environment leading to improvement in the different properties (swelling-adsorption) of the prepared hydrogel. To demonstrate the modification step, various techniques, including SEM, XRD, FTIR, TGA, and EDS, were used to characterize the prepared PAm@P hydrogel. Also, Different parameters affecting the adsorption processes were studied. The experimental data were analyzed with isotherms, kinetic, and thermodynamic models to study the removal performance of MB-dye PAm@P hydrogel. The selectivity, regeneration, and application of the prepared hydrogel were investigated to evaluate the adsorption performance of the PAm@P hydrogel.

Experimental procedure

Materials

Acrylamide (Am) (spectrum), N, N'-Methylenebisacrylamide (BIS) (99%), Potassium persulfate (PPS) (99%), Sodium hydroxide (99%), trisodium phosphate (99%), and methylene blue (99%), Rhodamine B (99%), E122 (99%), were obtained from Sigma-Aldrich, Munich, Germany. All chemicals and reagents were used without any further pretreatments.

Preparation of polyacrylamide- phosphate (PAm@P) hydrogel

For preparation of PAm, in a 250 mL glass beaker, 150 mL of distilled water was added, and then 5.0 g of acrylamide was dissolved using a magnetic stirrer. After complete dissolution, 0.25 g BIS was charged to the previously prepared solution under continuous stirring. Thereafter, 0.5 g PPS was mixed with the prepared mixture, and the reaction temperature rose to 80 °C till gelation. The obtained gel was treated with a homogenizer to convert the bulk gel into a microgel. For the preparation of PAm@P hydrogel, 22.0 g of Na_3PO_4 was dissolved in 500 mL of distilled water. Then, the PAm microgel previously prepared was added to the Na_3PO_4 solution and then refluxed and transferred into a Teflon-lined stainless-steel autoclave and heated at 180 °C for 4.0 h under autogenous pressure. The gel was filtered and washed with double-distilled water three times to remove unreacted species. Finally, the produced gel (PAm@P) was lyophilized and stored for characterization and further use., as summarized in Scheme 1. PAm@P hydrogel was prepared in three independent batches under identical experimental conditions.

Point of zero charge

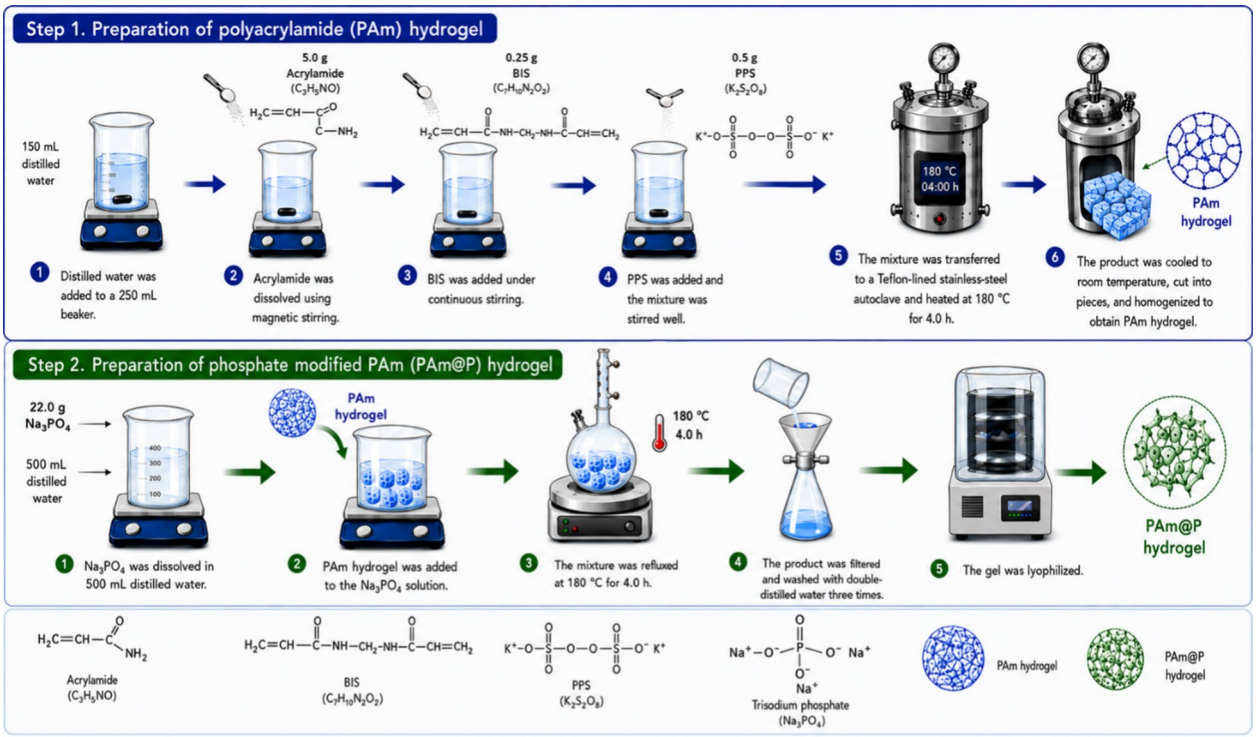
To determine the point of zero charge of PAm@P hydrogel. Initially, 10 mL of 0.01 M NaCl solution was adjusted to different pH values in the range (2–12). Then, 0.04 g of PAm@P were added to the previously solutions and let to shake for 48 h. thereafter, the solution filtrated and the final pH for each solution was measured. A relation between ΔpH (pH_f– pH_i) and pH_i was plotted and the point of zero charge was determined at the intersection of the curve with X-axis.

Characterization

Characterization of PAm and PAm@P hydrogels were investigated using various characterization techniques as discussed in the Supplementary Materials (Sect. 2.4).

Batch tests

Batch adsorption studies of MB dye by the PAm@P hydrogel at λ_{max} = 662 nm were investigated and discussed in the Supplementary Materials (Sect. 2.5).



Scheme 1. Preparation of polyacrylamide- phosphate (PAm@P) hydrogel.

Swelling studies

To estimate the ability of the fabricated PAm@P hydrogel to absorb water, 0.01 g of each gel were immersed in 25 mL distilled water and shake for 180 min. at different interval periods, the gel filtrated, dried with a wipe, and weighed. We followed the weights of the swollen gel until it reaches equilibrium. The swelling ratio was determined from Eq. (1a).

$$\%S = \frac{weight\ of\ swelling\ gel - weight\ of\ dry\ gel}{weight\ of\ dry\ gel} \times 100 \tag{1a}$$

To determine the swelling properties of PAm@P hydrogel at different pH values. 0.01 g of the dried gels were added to aqueous solutions of different pH values (2.0–9.0) and shaken for 5.0 min. At the end of the time, the weight of the swelling gels was determined, and %S was calculated as previously mentioned.

All adsorption and swelling experiments were repeated independently, and all measurements were performed in triplicate.

The selectivity factor (SF) of the investigated dyes was calculated as in Eq. (1b):

$$SF = \frac{\%R\ (MB - dye)}{(\%R\ (X)dye)} \tag{1b}$$

Where %R (MB-dye) is the experimental removal efficiency of MB-dye and %R (X)dye is the from the experimental removal efficiencies of the investigated dye (Rhodamine B or E122).

Mathematical modeling

Adsorption Isotherm, Kinetic, and Thermodynamic models applied in this work were given in the Supplementary Materials (Sect. 2.7.1–2.7.3, respectively) and Table S1.

Results and discussion

Characterizations

Swelling of super-adsorbent hydrogels

The water absorption capacity of the PAm@P hydrogel has a vital influence on its adsorption performance toward MB dye in aquatic media. The swelling properties can improve the surface area of the PAm@P hydrogel. Consequently, the adsorption efficiency will be enhanced compared with PAm[33]. The PAm@P hydrogel possessed a slow swelling rate (≈ 300%, 5.0 min). Thereafter, PAm@P exhibited an initial swelling ratio of approximately 300% within 5 min. The swelling ratio then increased sharply to about 3500% after 15 min and continued rising to approximately 6100% at 60 min. Beyond this time, equilibrium behavior was observed up to 180 min (Fig. 1a). Furthermore, the swelling percentage (%S) of PAm@P hydrogel was significantly affected by the pH

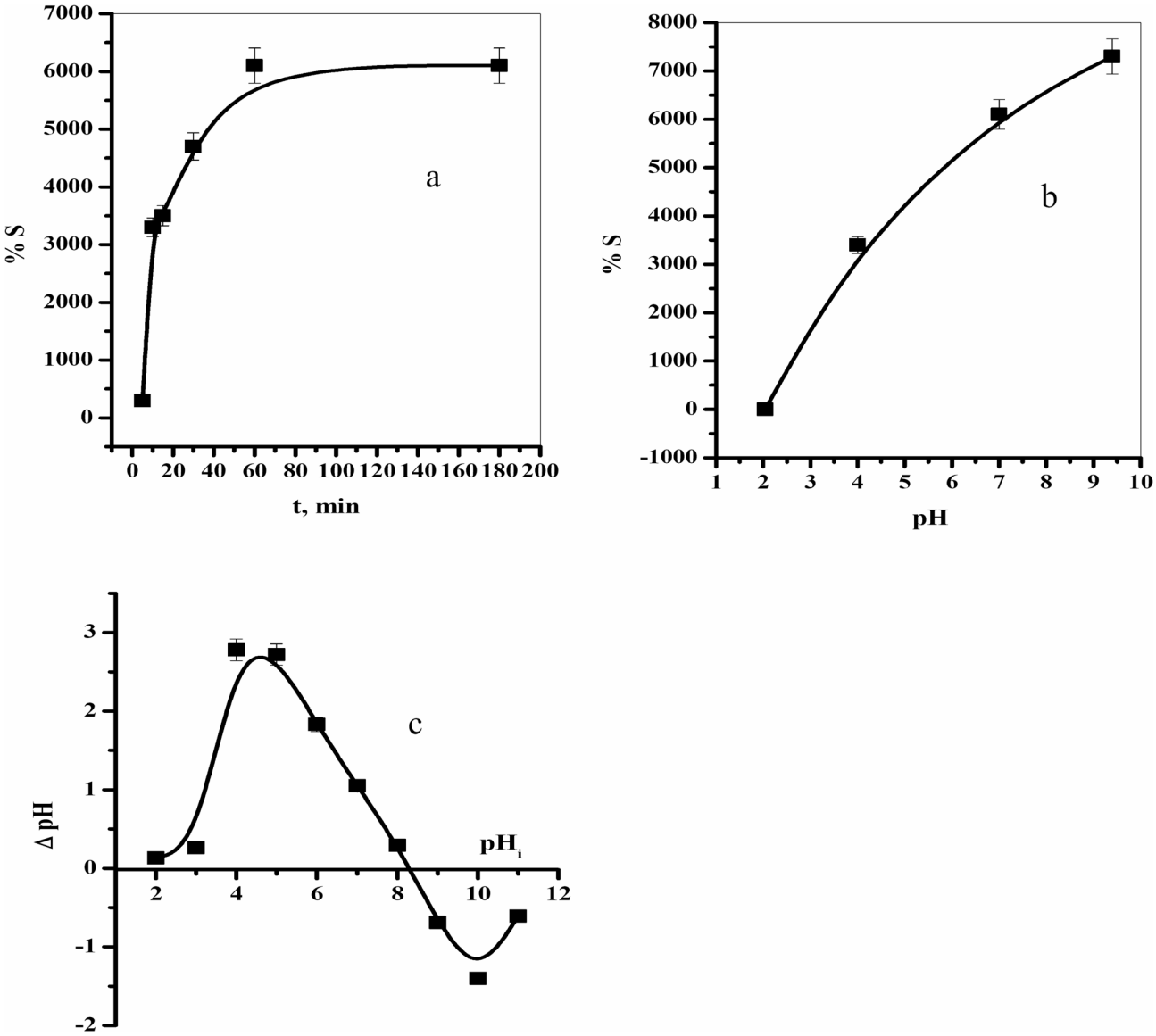


Fig. 1. Effect of (**a**) time, (**b**) pH, and (**c**) point of zero charge on the swelling percentages of PAm@P hydrogel.

of the aqueous medium, as represented in Fig. 1b. The swelling efficiency increased linearly (from 0 to 6000%) with pH values ranging from 2.0 to 7.0 and then increased slowly to (%S = 7000) with further increases in pH to 9.5. At alkaline pH, the carboxylic acid and phosphate functional groups of the fabricated PAm@P hydrogel are progressively deprotonated, increasing the density of negatively charged sites within the polymer chains. The enhanced electrostatic repulsion between these negatively charged groups promotes expansion of the hydrogel matrix and enlargement of its pore structure, facilitating water molecules diffuse more readily into the hydrogel matrix[20]. As a result, the swelling percentage (S%) increases under highly basic conditions, as illustrated in Fig. 1b. On the other hand, the higher swelling ratio (~7000%) of PAm@P hydrogel demonstrating its excellent water absorption capacity. Such extensive swelling generates a highly hydrated three-dimensional (3D) systems with enlarged free volume, facilitating the diffusion of MB molecules from the solution into the interior of PAm@P hydrogel. The swollen structure also exposes a greater number of amide ($-CONH_2$) and phosphate ($-PO_4^{3-}$) functional groups that serve as active binding sites. The improved diffusion characteristics, together with the increased availability of active adsorption sites, enhance the interaction between PAm@P hydrogel and MB molecules, resulting in superior adsorption capacity and adsorption efficiency. Therefore, the high swelling ratio plays a critical role in improving both the adsorption rate and the maximum adsorption capacity of the PAm@P hydrogel.

Point of zero charge

The value of the point of zero charge (pH_{pzc}) for the prepared PAm@P hydrogel was measured and represented in Fig. 1c. pH_{pzc} can indicate the reason for the alteration in the adsorption efficiency with pH values. The experimental results demonstrated that, at pH equal to pH_{pzc} =8.2, the adsorbent PAm@P hydrogel surface is

neutral (zero charged) while under acidic conditions ($pH < pH_{pzc}$), the surface of the prepared PAm@P hydrogel will be positively charged, which will be unavailable for interaction with positively charged MB molecules, leading to low adsorption efficiency. This behavior could be explained by the competition between H+ ions in the aqueous environment and MB dye for interaction with the adsorbents' active sites[34,35]. Conversely, when $pH > pH_{pzc}$ (> 8.2), the surface of the PAm@P hydrogel adsorbent becomes free of H^+ ions and has more negatively charged functional groups, which are appropriate for interaction with the positively Charged cationic MB dye[35,36]. This behavior can be attributed to fact that the PAm@P hydrogel contains phosphate ($H_2PO_4^-$ / HPO_4^{2-}/ PO_4^{3-}) and amide ($-CONH_2$) functional groups. At acidic pH, these functional groups are predominantly protonated, resulting in reduced surface charge density and therefore a less negative (or near-neutral) zeta potential. Under these conditions, electrostatic repulsion within the polymer network is minimized, leading to a more compact structure and lower swelling capacity. At higher pH values, deprotonation of these functional groups increases the density of negatively charged sites on the surface and within the bulk network. This leads to a more negative zeta potential, while simultaneously enhancing electrostatic repulsion between polymer chains and promoting osmotic swelling due to counterion influx. As a result, the PAm@P hydrogel exhibits increased swelling ratios under alkaline conditions[32–36].

Scanning electron microscopy (SEM)

SEM images of the prepared adsorbent before and after modification are presented in Fig. 2. At low magnification, pristine PAm exhibited a relatively homogeneous polymeric morphology composed of micrometer-sized particles with smooth surfaces, as shown in Fig. 2(a–b). At higher magnification, the particles appeared compact and featureless, without noticeable surface roughness or porosity (Fig. 2(c–d))[25]. Following phosphate modification, the morphology of the hydrogel changed markedly. The PAm@P hydrogel exhibited irregularly shaped agglomerated particles with fractured surfaces, as shown in Fig. 2(e–f). Higher-magnification images (Fig. 2(g–i)) revealed a rough and granular surface texture, indicating that the modification process altered the surface morphology and increased its heterogeneity. After adsorption process of MB, the PAm@P–MB composite showed that the surface remained rough and granular, while the presence of small surface deposits and partial coverage of the adsorbent surface suggested the attachment of dye molecules onto the hydrogel surface. These morphological changes are consistent with the successful adsorption of MB molecules by the fabricated PAm@P hydrogel, as illustrated in Fig. 2(j–l).

Fourier transform infrared analysis (FT-IR)

The FT-IR analysis of the PAm hydrogel, as shown in Fig. 3a, shows a characteristic stretching peak at 3349 cm^{-1}, assigned to the NH_2 group[23,25]. Also, it shows the characteristic bands at 3178 cm^{-1} (N-H bending vibration), 2925 cm^{-1} (aliphatic tensile peak, due to the presence of PAm in the hydrogel)[9], 1648 cm^{-1} (C = O stretching vibration), 1594 cm^{-1} (H_2O bending vibration), 1407 cm^{-1} (C-N stretching vibration), 1070 cm^{-1} (NH_2 bending vibration)[37–39], 910 and 670 cm^{-1} (N–H wagging)[4,23]. The existence of amine functional groups, in addition to amide and alcohol groups, indicates the formation of strong H-bonds[25]. After modification of PAm microgel by phosphate to fabricate PAm@P hydrogel in aqueous solution, the phosphate groups tend to bind with the microgel at the amine groups. Also, characteristic peaks were observed at 1162 cm^{-1} (P = O) and other bands appearing at 869 cm^{-1} owing to the P-O-C bonds[38]. On the other hand, the bands belonging to the amine groups (3178 and 1108 cm^{-1}) had disappeared, and the bands at 2925 and 1407 cm^{-1} shifted to 2937 and 1403 cm^{-1}, respectively. Also, other bands at 3349, 1648, 1594, 1307, 1202 cm^{-1} had a great shift to 3288, 1662, 1555, 1350, 1173 cm^{-1}. Moreover, new characteristic bands attributed to phosphate groups had appeared at 1099, 1015, 967 and 579 cm^{-1} which confirm the fabrication of PAm@P hydrogel. After adsorption of MB-dye by the prepared PAm@P hydrogel from aqueous solution, the active sites of PAm@P hydrogel covered by MB molecules and therefore many of characteristic absorption peaks related to the PAm@P hydrogel were shifted to 3267, 2941, 1803, 1702, 1532, 1493, 1459, 1249, 1203, 1162, 992, and 502 cm^{-1} which indicate the adsorption process. In addition to the major distinction spectra for MB-dye-FT-IR which appeared as intense and broad peak in region 3000–3650 cm^{-1} assigned to the vibration of bonded -OH groups with -N atoms of MB-molecules heterocycle and of unsaturated $(CH_3)_2$, (N-$(CH_3)_2$), groups[39], as well as other characteristics absorption peaks of MB-dye[39].

Thermogravimetric analysis (TGA)

TGA of pure PAm microgel showed three weight-loss phases, as shown in Fig. 3(b) and (c). Initial decomposition is observed at 32–157 °C (weight loss = 12.5%) and is seen in almost any hydrogel, attributed to the evaporation of moisture and interfering water[1,32]. The second stage occurs between 236 and 331 °C (weight loss = 14.63%) due to the decomposition of amide groups from carboxylate groups in the PAm chain[1]. The final stage of thermal decomposition was observed in the range of 331–800 °C (weight loss = 55.82%), which coincides with the carbonization of the main structure, leaving a residue of 15.5% (Fig. 3b). The modification of PAm with phosphate can introduce phosphate functional groups and phosphate-containing linked structures within the polymer network, as represented in Fig. 2(e-i). This behavior increases the amount of water adsorbed and interlayer water. Therefore, at 31–281 °C, the weight loss ratio was 25.8% due to the presence of the PO_4^{-3} group, which can form H-bonds with more H_2O molecules. On the other hand, the interaction between the phosphate and amine groups reduces the amount of ammonia released (at 281–392 °C, with a weight-loss ratio of 4.8%). Furthermore, the formation of these nanoparticles insulates the polymer molecule from heat, thus protecting it from further thermal degradation (331–800 °C, weight loss ratio = 18), resulting in a residue ratio of 50% (Fig. 3b). These results primarily demonstrate the high thermal stability of the prepared PAm@P hydrogel up to the degradation onset temperature, which is significantly higher than the investigated sorption operating conditions. This confirms that the investigated adsorption process of cationic dye molecules by the fabricated PAm@P hydrogel material occurs safely at room temperature without any risk of thermally induced

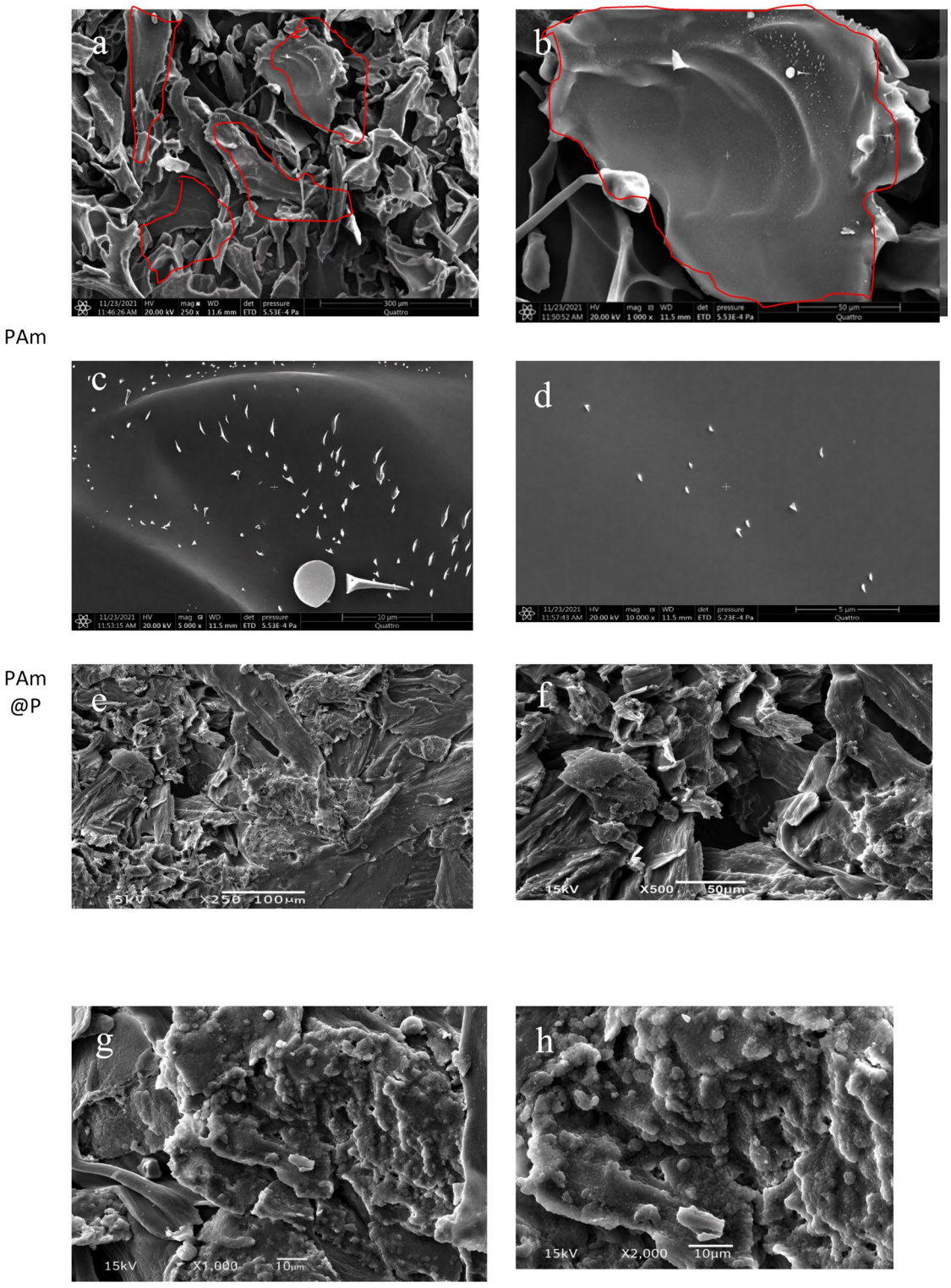


Fig. 2. Images of SEM of the PAm (**a**–**d**), PAm@P hydrogel (**e**–**i**), and PAm@P-MB (**j**–**l**) at different magnifications, respectively.

degradation, where thermal degradation is not expected under normal operating conditions. After adsorption of MB molecules onto the PAm@P hydrogel, MB molecules adsorb onto the active bonding sites on the PAm@P hydrogel surface. This reduces the thermal stability of PAm@P-MB compared to PAm@P hydrogel (28–287 °C, % wt loss = 29.00; 287–392 °C, % wt loss = 9.00; 392–800 °C, % wt loss = 35). This is attributed to the decomposition of a large quantity of MB molecules bonded to active sites of PAm@P hydrogel surface, with the remaining amount of adsorbent material (27%), as shown in Fig. 3 (b and c).

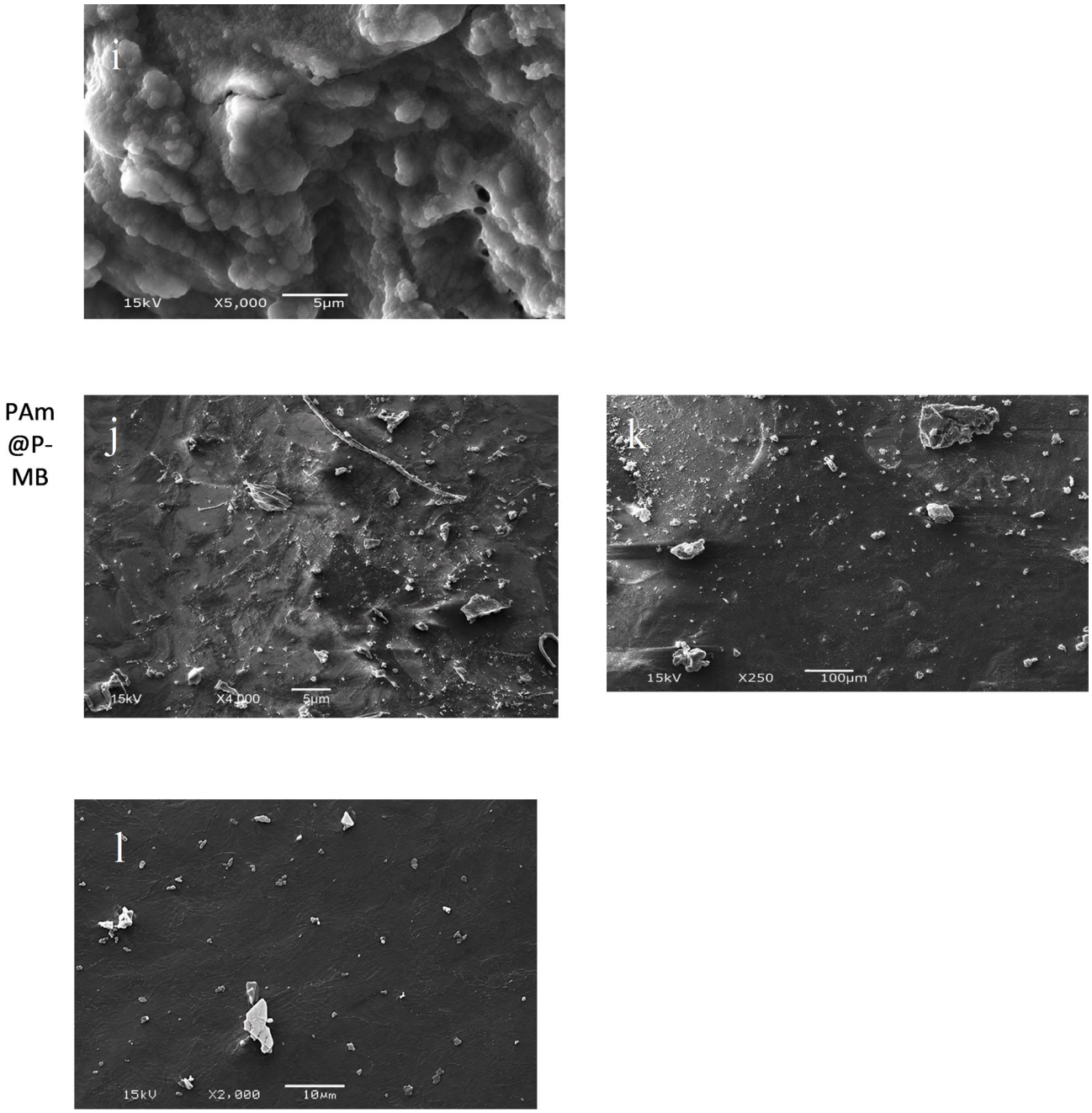


Fig. 2. (continued)

Energy-dispersed X-ray analysis (EDS)

EDS is a method used to analyze the energy of X-ray particles and is an effective technique for detecting the elemental composition of materials. As reported in our previous work[33], PAm is mainly composed of C, O, and N. By reacting PAm with phosphate in an aqueous environment, the phosphate groups bind to the PAm gel to form PAm@P hydrogel. Consequently, sodium and phosphorus are detected in the EDS analysis of PAm@P hydrogel, as illustrated in Fig. 4a. Therefore, EDS analysis confirmed the fabrication of PAm@P hydrogel. After adsorption of MB-dye onto PAm@P hydrogel active binding sites, the EDS analysis reveals the presence of S and Cl elements, which confirm the adsorption of MB molecules onto PAm@P hydrogel surface, as demonstrated in Fig. 4b. These elemental changes suggest the presence of MB molecules on PAm@P hydrogel surface suggesting successful uptake of the dye. However, it should be noted that EDS analysis is limited to elemental identification and cannot provide direct information regarding adsorption mechanisms or the nature of binding interactions; therefore, the observed elemental changes results are interpreted solely as supporting evidence of MB dye uptake.

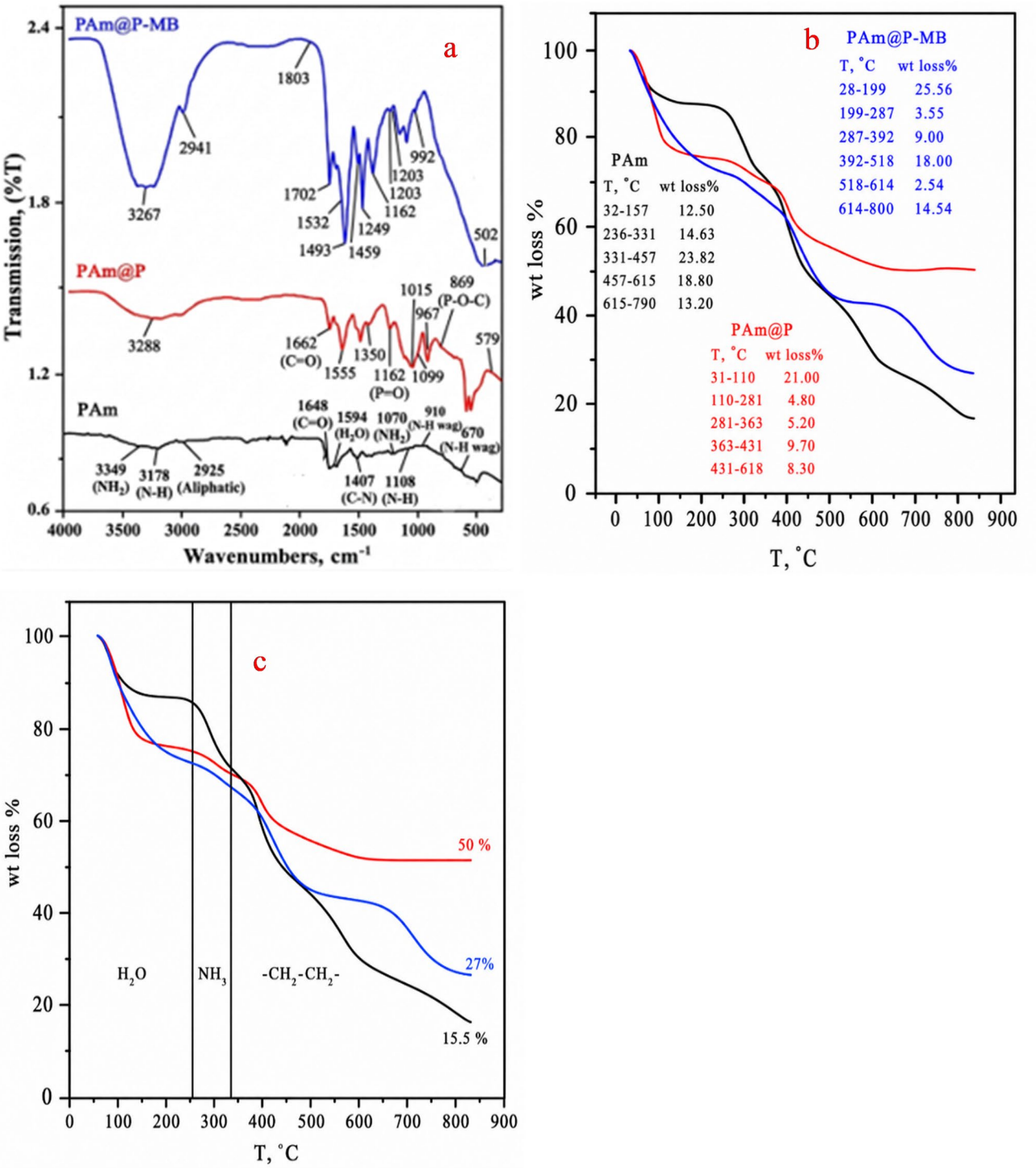


Fig. 3. (**a**) FTIR of PAm, PAm@P, and PAm@P-MB. and (**b**, **c**) TGA of PAm, PAm@P, and PAm@P-MB.

Adsorption experiment results

Effect of pH

The influence of the MB-dye solution pH on the sorption performance of PAm@P hydrogel was studied, as shown in Fig. 5a. It was observed that the sorption efficiency rapidly increased (0-96.23%) with increasing pH from 2.0 to 6.0. Thereafter, the removal percentage changed slowly (96.23–99.40%) with further increase of the pH value from 6.0 to 9.0 and then decreased with increased pH from 9.0 to 11.0 (99.4%-86.33%). This is referred to, at strongly acidic conditions (pH 2.0–4.0), the phosphate groups are highly protonated, while the amide groups remain essentially non-ionizable over the investigated pH range. The abundance of H^+ ions compete with MB molecules for the available active sites of PAm@P hydrogel, and the positively charged surface generates

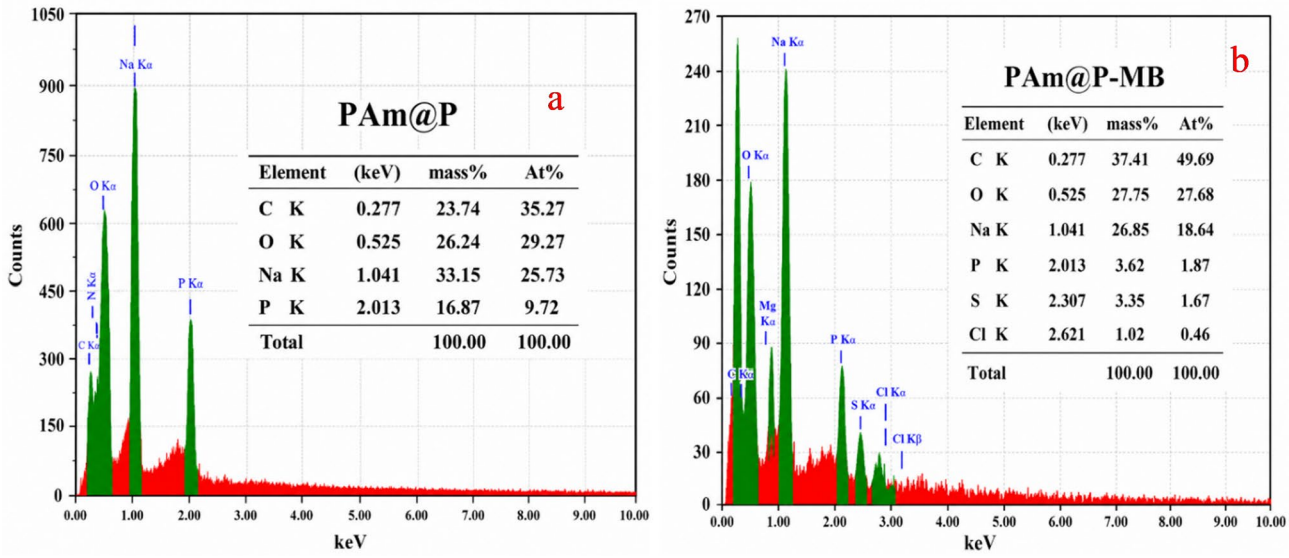


Fig. 4. The EDS analyses of (**a**) PAm@P hydrogel, and (**b**) PAm@P-MB-dye.

electrostatic repulsion, resulting in poor removal performances and very low adsorption efficiency. On the other hand, with increasing the pH toward neutral conditions, progressive deprotonation of the phosphate groups produces negatively charged phosphate species which improve the electrostatic attractions between the PAm@P hydrogel surface and the positively charged MB molecules. Simultaneously, the reduced competition from H^+ ions allow more active sites to become available, leading to the sharp increase in %R from 0.0% to >99% with increasing in pH from 2.0 to 8.2. Although the pH exceeds the pH_{PZC} (>8.2), there was only a slight increase in removal percentages reaching a maximum %R of 99.40% at pH 9.0. This behavior suggests that most active sites become occupied near neutral pH and further increases in surface negativity provide only a limited additional benefit[32–36]. Under highly alkaline conditions (pH 9.0–11.0), %R reduces to 86.33%. This reduction can be attributed to changes in the PAm@P hydrogel network caused by extensive deprotonation of phosphate groups, increased ionic strength, and competition between hydroxide ions (OH–) and MB molecules for the adsorption sites. Consequently, despite the negatively charged surface, the adsorption performance of PAm@P hydrogel decreases at very high pH values. The observed adsorption behavior is consistent with the acid-base properties of phosphate groups, whose reported literature pKa values govern their protonation and deprotonation over the investigated pH range. Although the pKa values of the prepared PAm@P hydrogel were not experimentally determined, the adsorption mechanism agrees well with the experimentally measured pH_{PZC} value of 8.2 and the expected ionization behavior of the phosphate functional groups[32–36].

Effect of MB-dye initial concentration

Figure 5b represented the influence of MB-dye initial concentrations versus sorption percentage by PAm@P hydrogel. It showed that the adsorption rate increased slowly with increasing initial MB-dye concentration, then decreased sharply with further increases in dye concentration. Also, the increasing in the initial MB dye concentrations from 50 to 300 mg L^{-1} caused a progressive improve in the equilibrium adsorption capacity (q_e) from 245.75 ± 3.24 to 1491.00 ± 7.68 mg g^{-1}. This behavior reflects the enhanced concentration gradient between the solution and PAm@P hydrogel surface, which increases the probability of collision between MB molecules and the available active sites, thereby promoting mass transfer and adsorption. Although the adsorption capacity continued to increase up to 300 mg L^{-1}, no further improvement was obtained at 400 and 500 mg L^{-1}, where q_e remained nearly slightly changed from 1491.25 ± 7.68 to 1490.00 ± 7.36 mg g^{-1}, respectively, as illustrated in Table 1. The negligible variation (<0.1%) demonstrates that the prepared PAm@P hydrogel had reached its q_{max} under the investigated conditions. Another important trend was observed for the adsorption performance of MB dye by PAm@P hydrogel, where more than 98% of MB molecules was adsorbed by PAm@P hydrogel over the concentration range of 50–300 mg L^{-1}, reaching a maximum %R of 99.5% at 200 mg L^{-1}. Moreover, the increasing in the initial concentrations beyond 300 mg L^{-1} resulted in a substantial decline in adsorption efficiency to 74.56% at 400 mg L^{-1} and 59.60% at 500 mg L^{-1}. Simultaneously, the equilibrium concentration (C_e) increased dramatically from 1.80 mg L^{-1} at 300 mg L^{-1} to 101.75 and 202.00 mg L^{-1} at 400 and 500 mg L^{-1}, respectively. This behavior can be attributed to the higher proportion and availability of adsorption active sites on PAm@P hydrogel to MB-dye at lower dye concentrations. This availability starts to decrease with increasing initial MB-dye concentrations, where the saturation and depletion of adsorption active sites, as well as the number of MB molecules, are highly exceeded over the number of binding sites[10]. Therefore, the adsorption active sites on PAm@P hydrogel will interact with a limited number of MB molecules and leave a high number of MB molecules in the solution. The removal results at various initial MB concentrations were fitted using Langmuir, Freundlich, Temkin, and Flory-Higgins models. The linear plots and data are calculated from Fig. 5 (c-f), and the calculated parameters are listed in Table 2. The calculated correlation coefficient (R^2) demonstrated

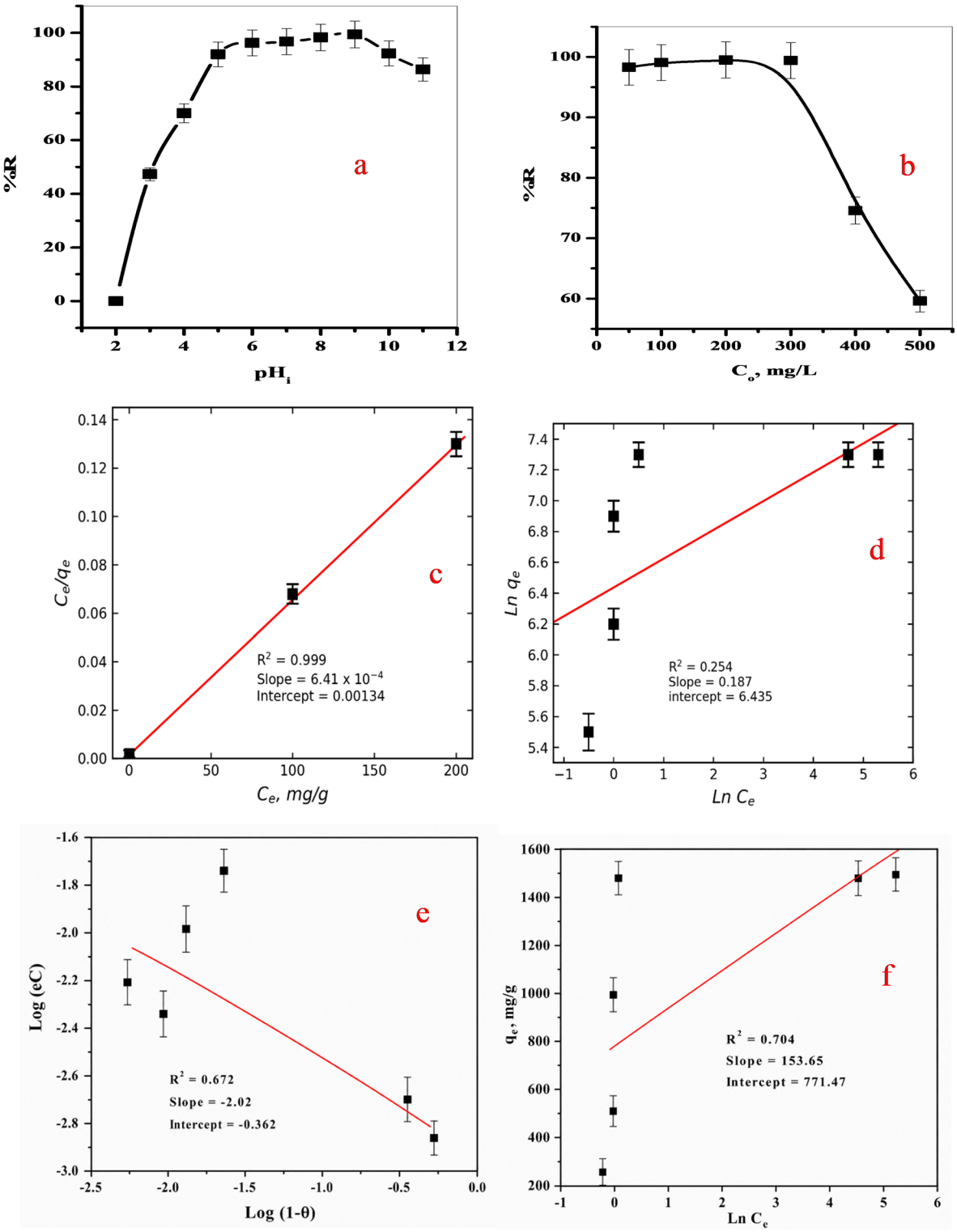


Fig. 5. Effect of: (**a**) pH(Dose = 0.005 g, t = 120 min, [MB] = 300 mg/L, T = 25 °C, v = 25 mL), (**b**) Initial MB-dye concentrations (Dose = 0.005 g, t = 120 min, pH = 7, T = 25 °C, v = 25 mL), adsorption isotherm plots of (**c**) Langmuir isotherm, (**d**) Freundlich isotherm, (**e**) Flory–Huggins isotherm, and (**f**) Tempkin isotherm of adsorption of MB-dye by PAm@P hydrogel.

that the removal of MB-dye by PAm@P hydrogel was best described with the Langmuir isotherm model, with R^2 of approximately unity (R^2 = 0.999). This indicated that MB molecules form a homogeneous monolayer with no interactions between molecules and adjacent sites with monolayer adsorption capacity (q_e) of 746.26 mg g^{-1}. Accordingly, from the values of the Langmuir isotherm constant (b = 2.1 L mg^{-1}), it can be concluded

C_i (mg L^{-1})	C_e (mg L^{-1})	*R*(%)	q_e(mg g^{-1})	C_e/q_e	lnq_e	LnC_e
50	0.85	98.3	245.75	0.00346	5.5	-0.1625
100	0.927	99.07	495.36	0.00187	6.05	-0.075
200	1.00	99.5	995	0.001	6.9	0
300	1.8	99.4	1491	0.0012	7.307	0.587
400	101.75	74.56	1491.25	0.068	7.3077	4.6225
500	202	59.6	1490	0.13	7.3065	5.3

Table 1. The relationship between initial MB dye concentration and other important adsorption parameters.

Isotherm Model	Parameters	Adsorbing dye
		MB
Langmuir	q_e(mg g^{-1})	746.26
	b (L mg^{-1})	2.1
	R^2	0.999
Freundlich	1/n	0.187
	K_F (mg g^{-1})	6.435
	R^2	0.254
Flory-Higgins	n	− 2.92
	K_{FH} (Lmol^{-1})	− 0.362
	R^2	0.672
Tempkin	B (J mol^{-1})	153.65
	A_T (L g^{-1})	771.47/153.65
	R^2	0.704

Table 2. Adsorption Isotherm study of MB dye by PAm@P hydrogel.

that the adsorption of MB onto Pam@P hydrogel is favorable. On the other hand, Freundlich isotherm model possessed lower correlation coefficient ($R^2 = 0.254$). The value of n related to the Freundlich isotherm model was 5.35 (> 1.0) indicating the physical nature, easier and more favorable dye adsorption[10,12]. Also, Flory-Huggins isotherm model was investigated to describe the degree of surface coverage characteristics of the adsorbate on the adsorbent. The Flory-Huggins isotherm possesses lower R^2 value (0.672), and Flory-Huggins equilibrium constant (K_{FH}) is (0.431 L mol^{-1}). Moreover, the lower value of R^2 (0.704) for the investigated Temkin isotherm model reveal that the adsorption of MB molecules by Pam@P hydrogel could not be described by this model. The heat of adsorption (B), the energy released during the interaction between the adsorbate and the adsorbent, plays a crucial role in the adsorption of MB dye by Pam@P adsorbent. Upon analysis of the acquired data, it was observed that the absorption temperatures were significantly high, indicating that the adsorption process will be physically and exothermic[10–12,18,20,32,40]. These findings indicated that the MB dye is uniformly adsorbed on the PAm@P surface as a monolayer, with a saturation capacity of 746.26 mg g^{-1}. This may be due to the presence of rich functional groups on the PAm@P hydrogel surface[10].

Effect of contact time

The effect of shaking time on the adsorption of MB-dye onto PAm@P hydrogel was studied, as shown in Fig. 6a, to determine the optimum time for effective adsorption of MB-dye using PAm@P hydrogel. Experimental results revealed that the adsorption rate of MB-dye onto PAm@P hydrogel was increased rapidly with increasing contact time till 60.0 min, ascribable to the availability of adsorption active sites on PAm@P hydrogel surface and the time required for MB-dye diffusion from bulk to hydrogel surfaces[10]. With further increase in the contact time (60.0–180.0 min), the adsorption rate of MB molecules by PAm@P hydrogel became constant. This may be attributed to the preferential occupation of all free active sites on the PAm@P hydrogel surface[15]. Pseudo-first-order kinetic (PFO), pseudo-second-order kinetic (PSO), liquid-film diffusion (FDM), and intra-particle diffusion kinetic models were investigated to describe the adsorption of MB-dye by PAm@P hydrogel. The linear equations of the applied models, linear relation and parameters were shown at Table S1, as represented in Fig. 6 (b-e), respectively.

The correlation coefficient (R^2) and other kinetic parameters calculated from the linear plots were recorded in Table 3. The PFO was employed to determine the adsorption rate constant, an initial model that characterizes the adsorption rate by accounting for adsorption capacity. PFO showed $R^2 = 0.976$, rate constant (k_1 = -slope = 0.055 min^{-1}) and the calculate adsorption capacity ($q_{e\,(Cal)}$) was 87.1×10^5 mg g^{-1}. The PSO hypothesis that the rate of MB molecules adsorption is directly proportional to the number of accessible adsorption sites on PAm@P hydrogel. From the data obtained in Table 3, the PSO shows R^2 value (0.999) that closely approximate unit. The experimental $q_{e(exp.)}$ (1536.1 mg g^{-1}) value shows a high degree of agreement with the calculated $q_{e(cal.)}$ (1491 ± 7.68 mg g^{-1}) value. Thus, it can be concluded that the PSO model is the best kinetic model for

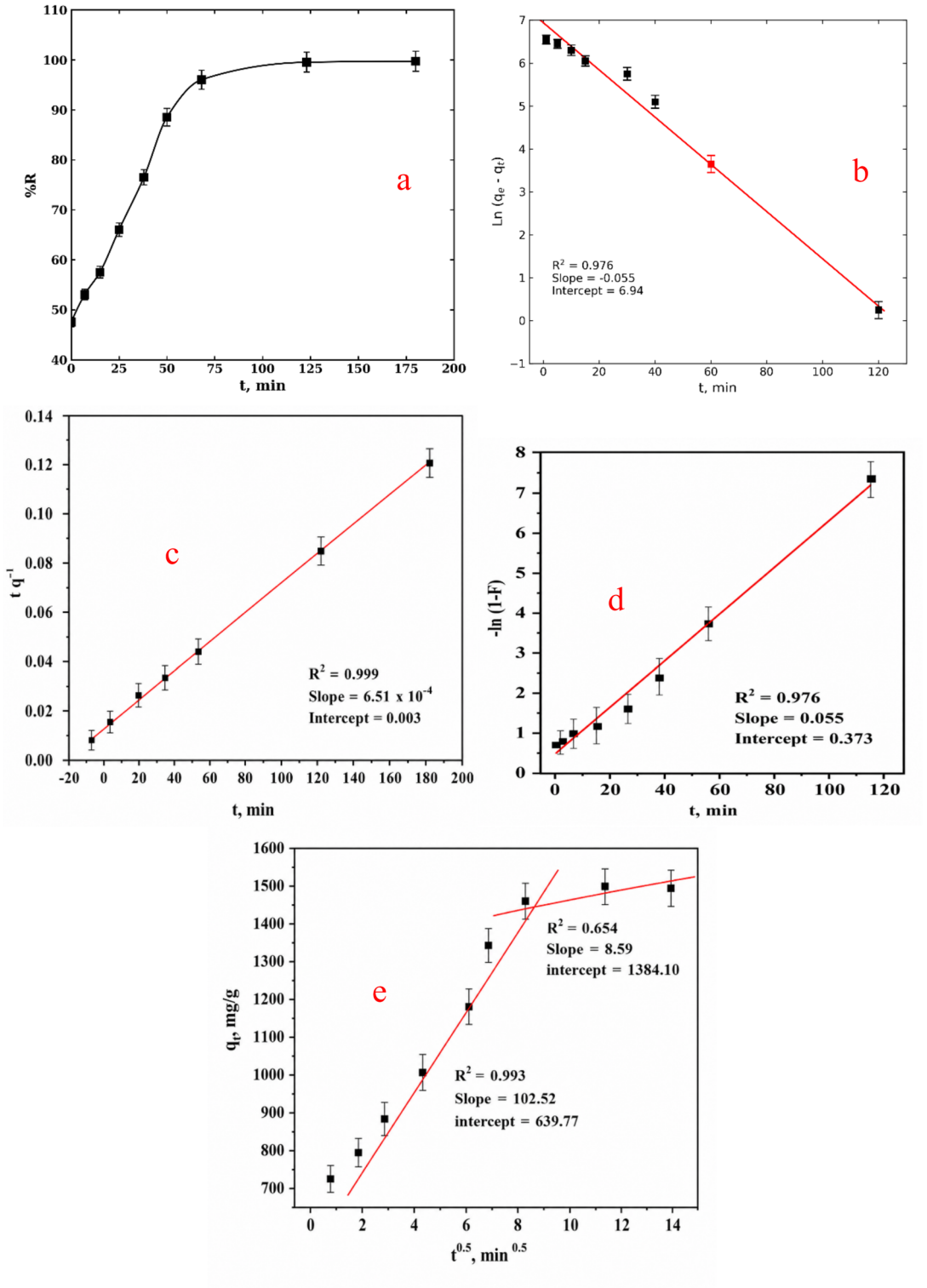


Fig. 6. (**a**) Effect of contact time on adsorption percentages of MB-dye by PAm@P hydrogel, (**b**) pseudo-first-order, (**c**) pseudo-second-order, (**d**) liquid-film diffusion, and (**e**) intra-particle diffusion kinetic models. (Dose = 0.005 g, pH = 9, [MB] = 300 mg/L, T = 25 °C, v = 25 mL).

describing the adsorption behavior of MB dye by PAm@P hydrogel. The film diffusion model (FDM) describes the process by which adsorbate molecules migrate through the liquid film surrounding the adsorbent particle. The FDM showed R^2 value of 0.976 with external film mass transfer coefficient K_{FD} = 0.055. These findings suggest that film diffusion is not the rate-limiting step in the overall adsorption kinetics. In addition, the intra-particle diffusion model revealed two-stage linear plots (Fig. 6c). In the first stage, the obtained large fitting

Kinetic Model	Parameters	Adsorbing dye
		MB
	$q_{e(Exp)}$ (mg g^{-1})	1491 ± 7.68
Pseudo first order	K_1 (min^{-1})	0.055
	q_e(cal.) (mg g^{-1})	87.1×10^5
	R^2	0.976
Pseudo-second order	K_2 (g $mg^{-1}min^{-1}$)	1.4×10^{-4}
	q_e(cal.) (mg g^{-1})	1536.1
	R^2	0.999
Liquid film diffusion	K_{FD}	0.055
	R^2	0.976
Interparticle diffusion		
STEP 1	C_1	639.77
	K_i1	102.52
	R^2	0.993
STEP 2	C_2	1384.10
	K_i2	8.59
	R^2	0.654

Table 3. Kinetic models of sorption of MB-dye by PAm@P hydrogel.

slope suggests fast diffusion rates in the adsorbent boundary layer, where MB molecules interact rapidly with the PAm@P hydrogel surface[6]. In the second stage, the lower efficiency related to lower diffusion rates due to gradual occupying the binding sites and diffusion resistance improvement[6]. The comparatively lower fitting of the PFO, film diffusion, and the two-stage intra-particle diffusion behavior, suggests that the adsorption process involves multiple mechanisms, including external mass transfer, intra-particle diffusion, and surface interactions. Thus, the obtained R^2 values indicate that the adsorption conforms to and is well fitted by the PSO, with a value close to unity and higher than that obtained for other investigated models[3,6,12,15]. This indicates that PSO best fits the adsorption of MB dye using the PAm@P hydrogel, and that the rate-limiting step may be chemosorption[15] as associated with adsorption processes involving surface interactions. Moreover, the theoretical equilibrium adsorption capacity (1536.1 mg g^{-1}) related to pseudo-second-order kinetic is highly close to the experimental value (1491 ± 7.68 mg g^{-1}). Therefore, the PSO model should be regarded as providing the best kinetic description of the adsorption process of MB molecules by PAm@P hydrogel from aquatic media rather than definitive evidence of chemisorption.

Effect of PAm@P hydrogel dosage

The PAm@P hydrogel dose is a critical factor affecting the hydrogel's adsorption performance. Figure 7a demonstrated the influence of hydrogel dosage on the sorption performance. With increasing PAm@P hydrogel dosage from 0.005 to 0.015 g, the sorption performance of MB-dye by the PAm@P hydrogel significantly increased. At low PAm@P hydrogel dosages, the number of binding active sites is limited and interacts with a low number of MB-dye, resulting in low adsorption efficiency. Whereas with increasing PAm@P hydrogel dose, the surface-active sites and functional groups that promote interactions with MB molecules increase, enhancing adsorption performance and thereby significantly increasing removal efficiency[6,10,40]. With further increasing PAm@P hydrogel dosage, the adsorption rate of MB-dye continued to slowly increase due to the number of binding sites exposed to MB-dye decreasing[6].

Effect of ionic strength

The impact of different interfering electrolytes on the adsorption performance of MB molecules by the prepared PAm@P hydrogel was investigated using 0.1 M NaCl, 0.1 M Na_2CO_3, and 0.1 M EDTA, as shown in Fig. 7b. The results clearly show that the removal efficiency of MB remains almost unchanged in the presence of all tested electrolytes, indicating a negligible influence of ionic composition on the adsorption process. Where, PAm@P hydrogel achieved removal percentages of about 97.9, 98.02, and 98.96% for NaCl, Na_2CO_3, and EDTA, respectively, demonstrating consistently high adsorption performance across different ionic environments. The very small variations observed are within experimental error and suggest that the adsorption process is only weakly affected by changes in ionic strength and the presence of carbonate or chelating species. Overall, the results presented in Fig. 7b confirm the excellent stability and robustness of PAm@P hydrogel toward interfering electrolytes and indicating that adsorption performance is not significantly affected by these common interfering species under the investigated conditions. This behavior indicates that the adsorption mechanism is not governed solely by simple electrostatic interactions but likely involves additional contributions such as hydrogen bonding and surface complexation, which help maintain high adsorption efficiency under varying aqueous conditions.

Effect of temperature

The impact of temperature on the sorption of MB-dye onto PAm@P hydrogel was investigated in the temperature range (25–45 °C). The results, as shown in Fig. 7c, revealed that as the temperature increased from 25 to 45 °C,

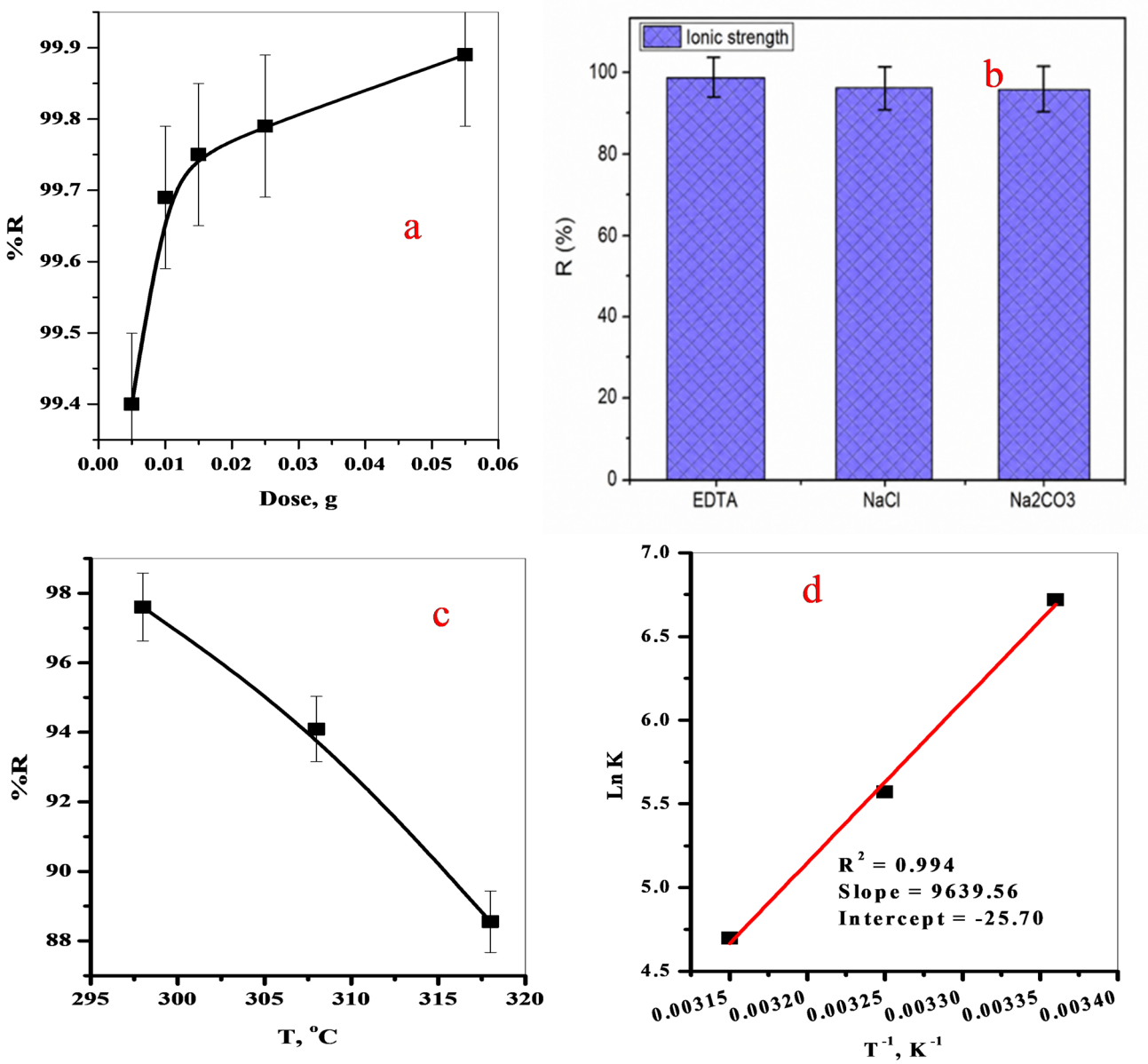


Fig. 7. Effect of (**a**) Adsorbent dose (t = 120 min, pH = 9, [MB] = 300 mg/L, T = 25 °C, v = 25 mL), (**b**) ionic strength (t = 120 min, pH = 9, [MB] = 300 mg/L, T = 25 °C, v = 25 mL), (**c**) temperature (Dose = 0.005 g, t = 120 min, pH = 9, [MB] = 300 mg/L, T = 25 °C, v = 25 mL), and (**d**) relation between ln K vs. 1/T on the adsorption of MB-dye onto PAm@P hydrogel.

Dye	T, K	ΔG°, kJ mol-1	ΔH°, kJ mol-1	ΔS°, J mole^{-1}K^{-1}
MB	298	− 16.65 ± 0.09	− 80.14 ± 2.9	− 213.65 ± 5.9
	308	− 14.27 ± 0.08		
	318	− 12.42 ± 0.06		

Table 4. Thermodynamic parameters of the sorption process of MB-dye by PAm@P microgel.

the sorption efficiency of MB molecules onto the PAm@P hydrogel decreased from 97% to 89%. This behavior can be explained based on the fact that at higher temperatures, the interactions between PAm@P hydrogel and the MB molecules are very low[42]. The different thermodynamic parameters were calculated from the linear relationship of Ln Kc vis T^{-1} (as represented in Fig. 7d) and summarized in Table 4. Where, the values of ΔH° and ΔS° were obtained from the slope and intercept, respectively, of the linear plot of ln Kc versus 1/T, as shown

in the Supplementary Materials (Table S1), and represented in Fig. 7d. While the Gibbs free energy change (ΔG°) was calculated using Eq. (2):

$$\Delta G^{\circ} = -RT \ln Kc \quad (2)$$

The calculated negative value of ΔH^0 (-80.14 kJ mol^{-1}) confirms that the investigated adsorption process of MB dye by PAm@P hydrogel is exothermic[41]. The negative value of ΔS° (-213.65 J mol^{-1} K^{-1}) suggests a decrease in randomness at the hydrogel–solution interface during adsorption, indicating a more ordered arrangement of MB molecules on the PAm@P hydrogel surface[18]. Furthermore, the negative ΔG° values at all investigated temperatures (-16.65, -14.27, and – 12.42 kJ mol^{-1} at 298, 308, and 318 K, respectively) indicate that the adsorption process is thermodynamically favorable within the investigated temperature range. It should be noted that these thermodynamic parameters were derived from measurements at only three temperature points (298, 308, and 318 K). Therefore, the calculated ΔH°, ΔS°, and ΔG° values should be regarded as approximate estimates rather than absolute thermodynamic constants. Nevertheless, the observed linear Van't Hoff relationship and the consistent trends of the calculated parameters provide reasonable evidence that MB adsorption onto the PAm@P hydrogel is predominantly governed by enthalpic effects over the investigated temperature range.

Desorption and recycling study

The reusability of adsorbent materials is a vital factor in evaluating their economic feasibility in practical applications. The regeneration tests were conducted by introducing the adsorbent in different solvents, MB (NaOH (0.5 M); HCl (1.0 M); Na_2CO_3 (0.5 M) and Ethanol) as desorbing agent for the MB-molecules from PAm@P hydrogel, as represented in Fig. 8 (a-c). It is concluded that 0.5 M NaOH achieves the highest desorption percentage among the materials used. Thereafter, different concentrations (0.1, 0.5, and 1.0 M) of NaOH were used, as shown in Fig. 8b. It was observed that 0.5 M NaOH showed the highest adsorption percentage, so it was used for further desorption experiments. As demonstrated in Fig. 8c, the adsorption/desorption efficiencies gradually declined over three regeneration cycles, which could be attributed to partial occupation of the binding sites due to strong interactions between the active sites and the dye molecules. PAm@P hydrogel exhibited good regeneration performance, maintaining its adsorption efficiency over repeated three cycles. The adsorption efficiency decreased gradually from 96.56% in the first cycle to 62.63% after the third cycle, indicating that approximately 64.9% of the initial adsorption efficiency was retained. Although the results obtained from the desorption and recycling study demonstrate that PAm@P hydrogel retains its adsorption performance after repeated use, detailed post-adsorption characterization was beyond the scope of the present study. Future work will focus on evaluating the structural and chemical stability of the adsorbent after adsorption using complementary characterization techniques.

Phosphate released from the fabrication process of PAm@P hydrogel, investigated adsorption process, and regeneration was not experimentally evaluated. Although the phosphate groups are grafted to the polymer network and are therefore expected to exhibit good chemical stability, quantitative assessment of phosphate leaching during adsorption and repeated regeneration cycles is necessary to fully evaluate the long-term performance and environmental safety of the adsorbent. This aspect will be investigated in future studies.

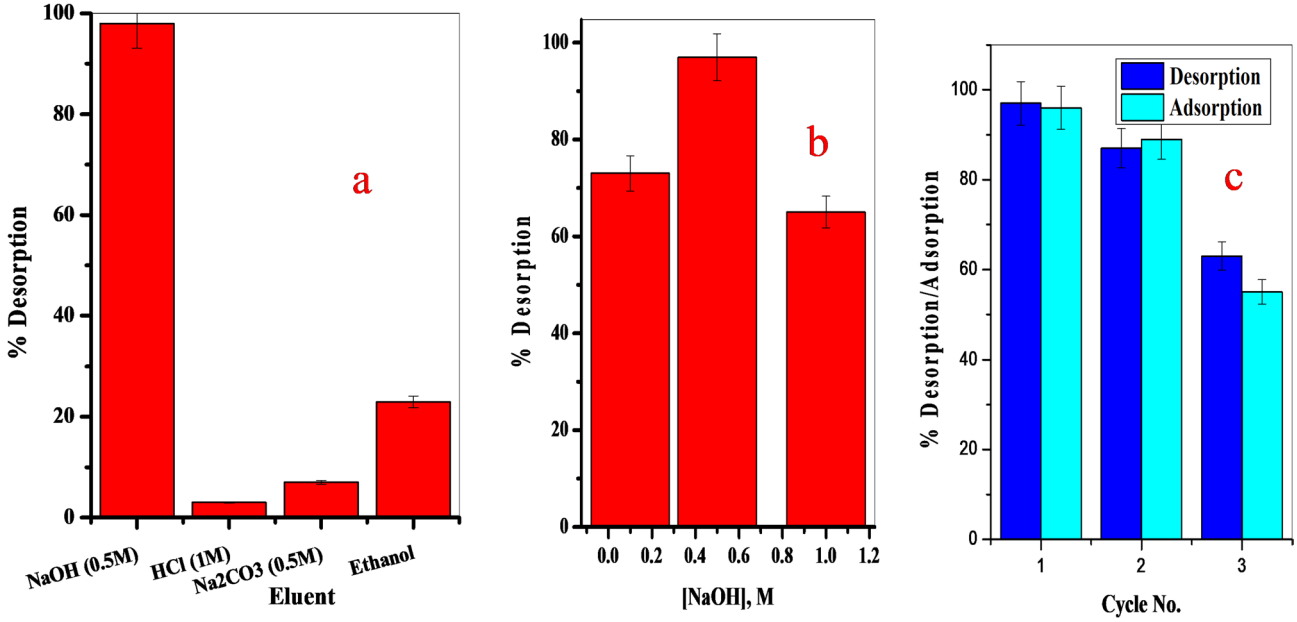


Fig. 8. Desorption of MB-dye using (**a**) different eluents, (**b**) different concentrations of NaOH eluent, and (**c**) adsorption-desorption behavior using NaOH 0.5 M as an eluent.

Adsorption selectivity

The selective adsorption of PAm@P hydrogel towards the MB-dye was further investigated by mixing MB with Rhodamine B and E122. The observations showed that the solution of the mixed dyes turned from the dark blue color, as illustrated in Fig. 9 (a and c), to a clear red color (as in Fig. 9 (b and d), which indicates selective removal of PAm@P hydrogel towards MB-dye from its mixture with Rhodamine B and E122. To quantitatively evaluate the adsorption performance of the prepared PAm@P hydrogel, the selectivity factor (SF) was calculated according to Eq. 1b. The calculated SF values were 2.31 for MB-dye over Rhodamine B and 3.10 for MB over E122, indicating a significantly higher affinity of the hydrogel toward methylene blue. These adsorption selectivity results demonstrate that the prepared PAm@P hydrogel illustrate a strong adsorption preference for MB dye even in the presence of other dyes. The successful selective removal of MB from binary dye mixtures containing Rhodamine B or E122 investigates that the hydrogel possesses high affinity toward MB dye, highlighting its potential wastewater treatment containing mixed dyes pollutants rather than single-dye systems. This selective behavior can be attributed to the favorable interactions between the active functional groups of PAm@P hydrogel and MB molecules. The selective adsorption of MB-dye over RhB may be attributed to the difference in molecular size, geometry, and diffusion behavior rather than charge effects, since both dyes are cationic under the experimental conditions. Although electrostatic interactions between the negatively charged functional groups of the hydrogel and both dye molecules facilitate uptake, MB exhibits higher sorption performances due to its smaller molecular size and planar structure, which enable easier penetration into PAm@P hydrogel and more effective access to internal active sites. Although the present study focused on representative binary dye mixtures, the obtained results provide promising evidence of the hydrogel's applicability in more complex wastewater systems. Further investigations involving additional cationic dyes and multi-contaminant systems will be conducted in future studies to comprehensively evaluate its practical performance under realistic environmental conditions. Although the investigated mixed-dye adsorption experiments by PAm@P hydrogel system clearly illustrates the preferential removal of the cationic dye, the present results should be regarded as qualitative evidence of adsorption selectivity. A comprehensive quantitative evaluation based on UV–Vis analysis of dye mixtures and selectivity coefficient calculations for such systems will be the focus of future investigations.

Application study

The adsorption performance of the PAm@P hydrogel was evaluated for MB-dye from real samples under the optimized experimental conditions. Under the optimized experimental conditions, calibration curves were prepared using treated standard solutions (1.0 L). The analytical samples were tap water (from labs at Mansoura University, Egypt), wastewater (from the Sinbellawin sewage station), and seawater from Ras-elbar City, Egypt. The experimental results were presented in Table 5. The chemical composition of the investigated real wastewater samples, including salt concentration and coexisting inorganic and organic species, was not analyzed in detail in the present work. Therefore, their possible effects on the adsorption performance were not evaluated. Further investigations involving complete chemical analysis of real wastewater samples will be conducted in future work to better understand the adsorption mechanisms under practical conditions.

Proposed adsorption mechanism of MB-dye on PAm@P hydrogel

The proposed adsorption mechanism of MB-dye onto the fabricated PAm@P hydrogel can be attributed to multi-interaction adsorption mechanisms involving electrostatic attraction, hydrogen bonding, pore diffusion, and surface complexation, as represented in Scheme 2. After phosphate modification, the fabricated PAm hydrogel contains abundant–$CONH_2$, –OH, and $-PO_4^{3}-$, groups. These groups increase the hydrophilicity of the fabricated PAm@P hydrogel and create a swollen, porous network, thereby facilitating the diffusion and entrance of MB molecules inside the hydrogel structure to be closely to the binding sites. At pH values around the pH_{pzc} of PAm@P hydrogel (pH = 5–9), the phosphate is almost completely ionized, producing negatively charged sites

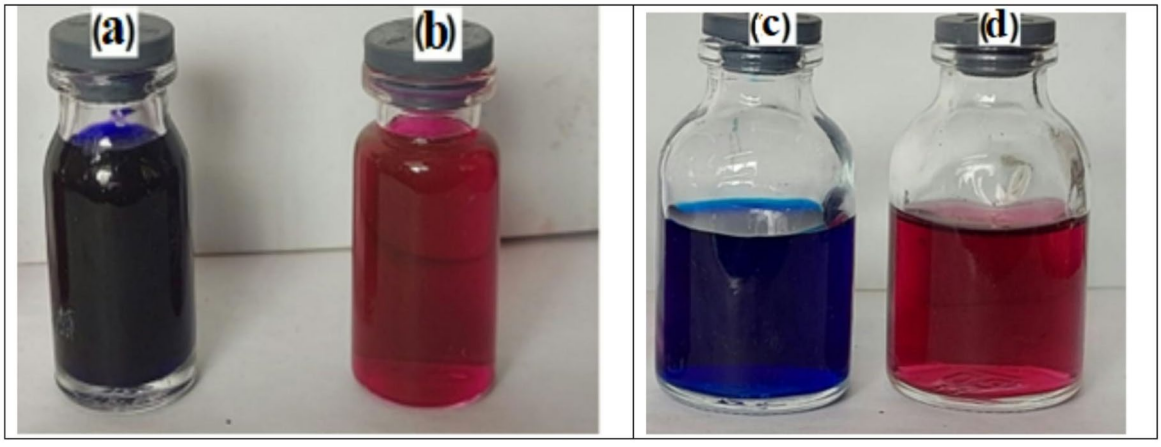
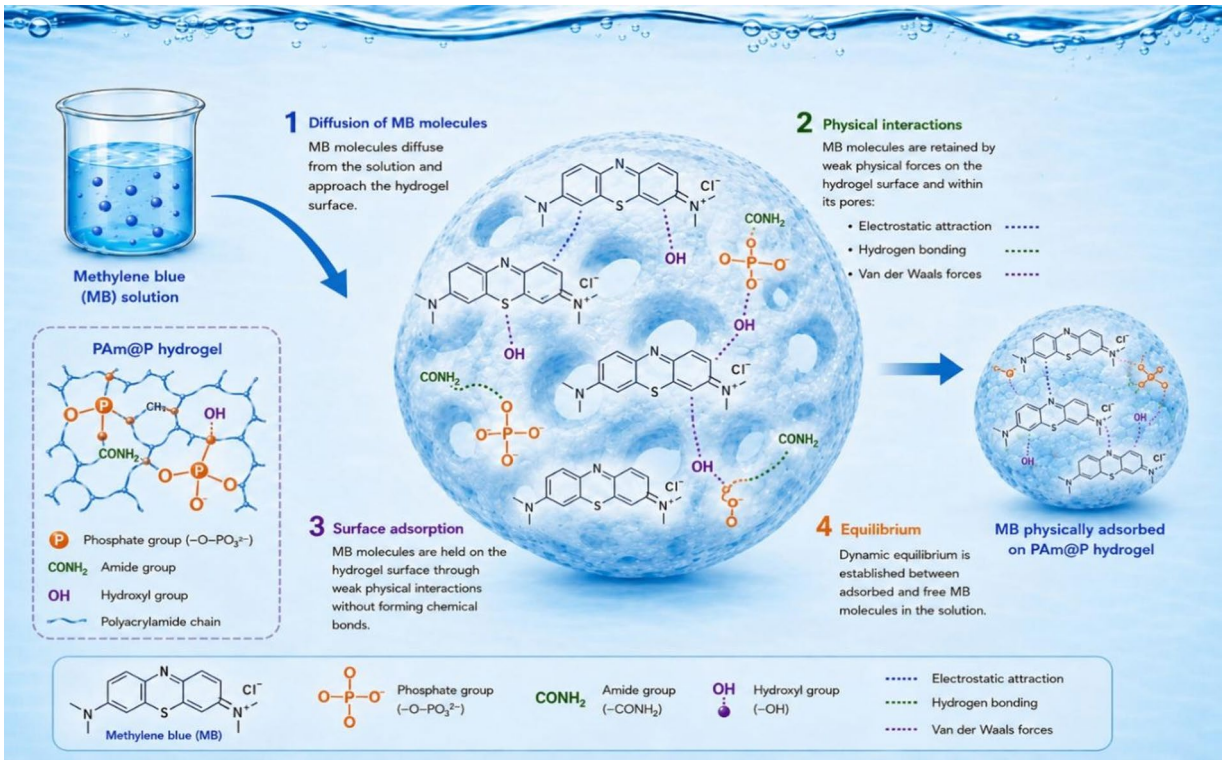


Fig. 9. Photographic image of Methylene blue and Rhodamine B mixture (**a**) before and (**b**) after treating with PAm@P hydrogel and Mix of MB and E122 (**c**) before and (**d**) after treating with PAm@P hydrogel.

Sample	Dye	Spiked (μg mL^{-1})	Measured (μg mL^{-1})	Recovered (μg mL^{-1})	Recovery (%)
Wastewater	MB-dye	0.00	0.00	0.00	0.00
		100	2.01	97.99	98.9
		300	10.93	239.07	96.93
Tap water	MB-dye	0.00	0.00	0.00	0.00
		100	1.34	98.66	99.586
		300	5.71	294.29	98.68
Sea water	MB-dye	0.00	0.00	0.00	0.00
		100	3.18	96.82	97.72
		300	18.84	281.16	94.28

Table 5. Analytical results of MB-dye adsorption (μg ml^{-1}) from real samples using PAm@P hydrogel.



Scheme 2. Proposed adsorption mechanism of MB-dye on PAm@P hydrogel.

such as $–PO_4^{3}–$. These negatively charged sites attract the positively charged MB molecules through electrostatic attraction and release Na^+. After adsorption of MB molecules by the prepared PAm@P hydrogel, additional peaks corresponding to S and Cl atoms on the EDS analysis of PAm@P-MB, as illustrated in Fig. 4b, which originate from the MB molecules, are clearly observed. The appearance of these characteristic elements after adsorption confirms the attachment of MB molecules to the PAm@P hydrogel. Moreover, the high adsorption capacity of PAm@P hydrogel towards the MB-dye was effect on the thermal stability of the obtained PAm@P-MB, as shown in Fig. 3c and b. Where, the PAm@P-MB presented lower thermal stability in all decomposition stages compared with PAm@P hydrogel and finally the residue in case PAm@P-MB (27%) almost half that obtained in case of PAm@P hydrogel (50%). Moreover, the FITR of PAm@P-MB presented intense bands compared with PAm@P hydrogel, as demonstrated in Fig. 3a. In addition, after the adsorption of MB molecules, the position of the many FTIR bands for PAm@P hydrogel had been shifted due to the interactions between MB molecules and the active sites on PAm@P hydrogel. The high adsorption performance of PAm@P hydrogel is primarily attributed to the presence of abundant phosphate and amide functional groups, which provide numerous active adsorption sites for MB molecules, in combination with its three-dimensional hydrophilic polymeric network that promotes efficient mass transfer. Although the SEM images reveal a porous and interconnected morphology, BET surface area and porosity measurements were not conducted in this study. Therefore, no direct correlation between adsorption performance and specific surface area is claimed. Future work will include BET surface area and pore size analyses to provide a more comprehensive understanding of the structure–adsorption relationship.

Adsorbent	Dose	pH	Equilibrium time	%*R*	Regeneration	q_{max}, mg g^{-1}	Refs.
PAm@P hydrogel	160 mg L^{-1}	7	60 min	99.3	3	1490	This study
Ni–polyacrylamide composite	30 mg L^{-1}	6.0	240 min	94	3	14.3	42
ZHC-4	400 mg L^{-1}	7.0	24 h	99	6	682.67	43
SA/PAM/PPy-TiO_2hydrogel	–	7.0	120 min	100	5		44
SCHMs	800 mg L^{-1}	10	180.0 min	99.4	5	64.05	45
Cs-STMP-ACM hydrogel	400 mg L^{-1}	10	10 min	85%	3	872	46
Hyd *Hyd/C30B* *C30B*	800 mg L^{-1}	8	30 min	–	–	67.11 77.51 70.42	47
HG *HG/BC* *HG/MTWBC*	1.5 g L^{-1}	8	70 min	83.22 92.57 94.27	–	12.3 14.2 20.79	48
PAAm/TP hydrogel	180 mg/25mL	7.0-8.5	600 min	82	5	0.57	49
Poly(AA-Co-NaAMPS) Hydrogel	240 mg L^{-1}	7	120 min	97	–	595.3	50
Fe_3O_4/poly(HEMA-co-AMPS) magnetic hydrogels	1.0 g L^{-1}	6.5	10 min	98.5	10	445.35	51
Hydrogel sodium alginate /Fe_3O_4	–	8	20 min	95	4	200	52
poly(HEMA-co-AMPS)/VAC	1.0 g L^{-1}	7	24 h	78.1	5	284.90	53
N-maleyl chitosan/P(AA-co-VPA)	50 mg L^{-1}	7	100 min	–	4	66.89	54
poly(AAm-co-AMPS)/Na-MMT hydrogel	50 mg L^{-1}	9	330–390 min	93	4	176	55
NAM@CuO NCs hydrogel	1.2 g L^{-1}	7	6.5 min	93.99	5	82.44	56
XGX-g-PAAHs@CuO nanocomposite	1.2 g L^{-1}	7	30 min	95.2	5	132.1	57
CNAM@Co_3O_4 NCs hydrogel	1.2 g L^{-1}	7	30 min	95.28	5	380.07	58
HAM@Co_3O_4 NCs hydrogel	1.6 g L^{-1}	7	30 min	94.91	5	294.64	59
PMH@CuO nanocomposite	1.2 g L^{-1}	7	30 min	98.41	5	132.27	60
VSi-CTS-g-PAAm hydrogel	1.0 g L^{-1}	12	24 h	98	–	68.02	61
porous alginate-based polyHIPE (AGA)	1.5 g L^{-1}	8	3 h	99	5	66.87	62

Table 6. Comparison of highest adsorption capacity q_{max} values of MB-dye by PAm@P hydrogel and other adsorbent materials[42–62].

Based on the results obtained in this work, it can be observed that the fabricated PAm@P hydrogel offers several advantages as an adsorbent to remove cationic dyes from environmental samples. The incorporation of phosphate functional groups provides considerable abundant negatively charged active sites, resulting in high adsorption performance and remarkable selectivity toward cationic dyes molecules through electrostatic attractions and surface complexation. PAm@P hydrogel also exhibits a 3D porous network that facilitates rapid diffusion of dye molecules and enhances removal efficiency. Furthermore, the preparation procedure is relatively simple and employs readily available monomers, making the material potentially suitable for scalable production. Despite these advantages, several limitations should be considered. The adsorption performance should be further evaluated using real industrial wastewater containing competing ions and mixed organic contaminants, in addition to an economic assessment of large-scale synthesis and application is necessary before practical implementation in wastewater treatment systems. Future work will focus on addressing these aspects to further demonstrate the feasibility of the prepared PAm@P hydrogel for real-world environmental applications. Also, the phosphate release from the chemically grafted PAm@P hydrogel was not experimentally evaluated. Although the phosphate groups are covalently attached to the polymer network and are therefore expected to exhibit good chemical stability, quantitative assessment of phosphate leaching during adsorption and repeated regeneration cycles is necessary to fully evaluate the long-term performance and environmental safety of the adsorbent. This aspect will be investigated in future studies. Although the adsorption–desorption results demonstrated satisfactory reusability of the hydrogel, detailed after regeneration characterization (e.g., FTIR, SEM, swelling behavior, and mechanical property analysis) was not performed in the present study. Such analyses will be the focus of future investigations to further verify the structural integrity and long-term stability of the regenerated hydrogel.

Comparison study

Recently, numerous types of adsorbents hydrogels have been investigated and published to eliminate MB-dye from aquatic media[42–62]. Adsorbent dose, pH, equilibrium time, removal percentages, and maximum adsorption capacity such adsorbents were reported in Table 6. Most of the adsorbents examined illustrate highest adsorption capacity (q_{max}) for MB-dye ranged 0.57–872 mgg^{-1}. Also, the data represented revealed that the fabricated hydrogel in this work has a considerable optimum conditions and maximum adsorption capacity compared with the published works as well as the fabricated PAm@P hydrogel still has many advantages and suitability for practical environmental applications.

Sustainability considerations

A qualitative sustainability assessment was conducted using a cradle-to-gate perspective, covering the production of raw materials, hydrogel synthesis, phosphate functionalization, purification, and drying prior to the adsorption stage. The PAm@P hydrogel is prepared in an aquatic media, thereby eliminating the use of volatile organic solvents and reducing solvent-related environmental hazards. The fabrication processes employ commercially available reagents and involve relatively few processing steps, contributing to good material utilization and minimizing additional processing requirements. However, the environmental footprint of the fabrication process is primarily influenced by thermal energy consumption during free-radical polymerization (80 °C) and the phosphate functionalization step (180 °C for 4 h), as well as water consumption during repeated washing and freeze-drying of the final product. From a life-cycle perspective, these stages are expected to be the dominant contributors to energy demand and associated greenhouse gas emissions. Although a complete quantitative Life Cycle Assessment (LCA) was not performed in this work, the present synthesis strategy demonstrates several features consistent with more sustainable material development, including the use of water as the reaction medium, the avoidance of hazardous organic solvents, efficient incorporation of phosphate functional groups, and the potential for adsorbent regeneration and repeated use. In addition, the regeneration and reuse capability of the PAm@P hydrogel, demonstrated in this study, can reduce material consumption and waste generation over multiple adsorption cycles, thereby improving its overall sustainability. Similar sustainability considerations and the importance of LCA for hydrogels and polymer-based adsorbents used in wastewater treatment have been highlighted in recent published works, emphasizing that solvent selection, energy consumption, regeneration efficiency, and system boundary definition are critical factors for evaluating the environmental performance of adsorption materials[63–65].

Cost evaluation and practical applicability of the PAm@P hydrogel

In addition to remove performance of the fabricated PAm@p hydrogel, its economic feasibility is important parameter for assessing its potential industrial applications in treatment technologies of wastewater. Accordingly, a preliminary cost evaluation of the prepared PAm@P hydrogel was investigated based on the approximate market prices of the raw materials used in its preparation. PAm@P hydrogel is synthesized from relatively inexpensive and commercially available materials, including acrylamide, N,N′-methylenebisacrylamide (BIS), sodium phosphate (Na_3PO_4), and a radical initiator, all of which are widely used in industrial polymer production. Moreover, the preparation processes are based on simple free-radical polymerization processes conducted under mild conditions, without requiring expensive catalysts, high-pressure systems, or energy-intensive processing steps, thereby reducing overall production costs. Based on current market prices of the precursors 18.6–20.0 USD kg^{-1}. This low cost is attributed to the use of inexpensive monomers and reagents, a straightforward aqueous polymerization process, and the absence of expensive catalysts or complex processing techniques. Considering the experimentally obtained adsorption capacity of 1490 ± 7.36 mg g^{-1} for methylene blue, the estimated cost of dye removal is approximately 12.5–13.5 USD per kg MB-dye removed, indicating favorable economic feasibility compared with many reported polymer-based adsorbents. Although this analysis suggests promising economic feasibility, a full techno-economic assessment including operational costs, regeneration performance, and large-scale manufacturing considerations, is necessary for a more accurate evaluation of industrial viability. Such detailed analysis is recommended for future investigations.

Conclusion

In this investigation, the modification of PAm with phosphate group was succeeded to yield PAm@P hydrogel. The modification step was confirmed with characterization with different advanced techniques. As a result, both swelling and adsorption properties of the new material (PAm@P) were improved compared with the original polymeric material (PAm). The adsorption parameters were best fitted with pseudo second order ($q_{e(cal.)} = 1536.1$ mg g^{-1}) and Langmuir adsorption isotherm ($q_e = 746.26$ mg g^{-1}). Thermodynamic analysis revealed that the adsorption process was spontaneous and exothermic, with $\Delta H° = -80.14$ kJ mol^{-1}, $\Delta S° = -213.65$ J mol^{-1} K^{-1}, and negative Gibbs free energy values ranging from – 16.65 to – 12.42 kJ mol^{-1} over the investigated temperature range, indicating that the adsorption process is primarily driven by enthalpic interactions. In addition, the experimentally determined q_{max} was 1490 ± 7.36 mg g^{-1} under the optimum adsorption conditions of an adsorbent dose of 0.005 g, initial MB concentration of 300 mg L-1, contact time of 120 min, solution pH 7, temperature of 25 °C, and solution volume of 25 mL. Moreover, the prepared PAm@P hydrogel showed suitable selective adsorptivity towards MB-dye in the presence of RhB and E122 with SF values of 2.31 for MB-dye over Rhodamine B and 3.10 for MB over E122, Moreover, PAm@P hydrogel can be reused for three cycles with acceptable adsorption percent. Practical applicability was verified through the treatment of real water samples, achieving high MB molecules recovery values of 96.93–98.90% for wastewater, 98.68–99.59% for tap water, and 94.28–97.72% for seawater. Overall, these findings demonstrate that the phosphate-functionalized PAm@P hydrogel is a highly efficient, selective, reusable, and environmentally promising adsorbent for the removal of cationic dyes from contaminated aquatic media, highlighting its strong potential for practical wastewater treatment applications.

Data availability

The authors state that the article contains all pertinent data needed to support the study's conclusions. The corresponding author can provide more information upon request.

Received: 12 May 2026; Accepted: 27 July 2026
Published online: 29 October 2026

References

1. Sharifi, K. M., Marjani, A. P. & Balkanloo, P. G. Enhanced dye removal using montmorillonite modified with graphene quantum dots in sustainable salep nanocomposite hydrogel. *Sci. Rep.* **14**, 7011. https://doi.org/10.1038/s41598-024-57729-0 (2024).
2. Rabeie, B., Mahmoodi, N. M. & Kazemian, H. Visible light assisted magnetic COF/HKUST/$CoFe_2O_4$ composite as a novel photocatalyst: green synthesis and efficient degradation of pollutants (dye and pharmaceutical) in water. *Adv. Compos. Hybrid. Mater.* **9**, 160. https://doi.org/10.1007/s42114-026-01696-9 (2026).
3. Rabeie, B. & Mahmoodi, N. M. Environmentally friendly novel covalent organic framework composites as porous photocatalysts and adsorbents for Tetracycline and dyes (Congo Red and Methylene Blue) removal: Green synthesis, kinetics, regeneration, and removal mechanisms. *Appl. Mater. Today*. **46**, 102884. https://doi.org/10.1016/j.apmt.2025.102884 (2025).
4. Mahmoodi, N. M. & Bagherzadeh, S. B. Synthesis of binary and ternary MOF/carbon based composites (MOF/ carbon nitride/ graphene oxide) for the visible-light assisted destruction of tetracycline and textile dye. *Nano Mater. Sci.* **7**, 359–376. https://doi.org/10.1016/j.nanoms.2024.04.015 (2025).
5. Koc, U., Aykut, Y. & Eren, R. High-strength and stretchable fabric-reinforced hydrogel composites: Their applications on the removal of methylene blue. *Fibers Polym.* **26**, 2147–2157. https://doi.org/10.1007/s12221-025-00938-9 (2025).
6. Kamal, S., Khalid, M., Khan, M. S., Shahid, M. & Ahmad, M. A bifunctionalised Pb-based MOF for iodine capture and dye removal. *Dalton Trans.* **52** (14), 4501–4516. https://doi.org/10.1039/d3dt00237c (203).
7. Shah, S. S., Ramos, B., Otubo, L. & Teixeira, A. C. S. C. Deep removal and photodegradation of methylene blue dye using superabsorbent polymer hydrogel composite with activated charcoal and TiO_2 nanoparticles. *ACS Omega*. **10**, 26441–26457. https://doi.org/10.1021/acsomega.4c11428 (2025).
8. Rabeie, B. & Mahmoodi, N. M. Green synthesis of biopolymer-driven dual functional carboxymethyl cellulose composite (CMC/ MIL100(Fe)/MIL88A(Al)) as a Z-scheme photocatalyst and an adsorbent for water pollutants. *Int. J. Biol. Macromol.* **329**, 147358 (). https://doi.org/10.1016/j.ijbiomac.2025.147358. (2025).
9. Chen, K. et al. Removal of methylene blue dye from aqueous solutions by pullulan polysaccharide/polyacrylamide/activated carbon complex hydrogel adsorption. *ACS Omega*. **8**, 857–867. https://doi.org/10.1021/acsomega.2c06205 (2023).
10. Hassan, A. F., El-Naggar, G. A., Esmail, G. & Shaltout, W. A. Efficient adsorption of methylene blue on novel triple-nanocomposites of potassium kappa-carrageenan, calcium alginate and nanohydroxyapatite obtained from sea scallop shells. *Appl. Surf. Sci. Adv.* **13**, 100388. https://doi.org/10.1016/j.apsadv.2023.100388 (2023).
11. Samrah Kamal, M. et al. Shabbir Ahmad, Synthesis, characterization and DFT studies of water stable Cd(II) metal–organic clusters with better adsorption property towards the organic pollutant in waste water. *Inorg. Chim. Acta*, **512**, 1198722020. https://doi.org/10.1016/j.ica.2020.119872
12. Aldahash, S. A., Higgins, P., Siddiqui, S. & Uddin, M. K. Fabrication of polyamide-12/cement nanocomposite and its testing for different dyes removal from aqueous solution: characterization, adsorption, and regeneration studies. *Sci. Rep.* **12**, 13144. https://doi.org/10.1038/s41598-022-16977-8 (2022).
13. Alharbi, K. H. Efficient removal of methylene blue from aqueous solutions using mixed oxides of cobalt oxide and tungsten trioxide modified graphene oxide. *J. Saudi Chem. Soc.* **28**, 101802. https://doi.org/10.1016/j.jscs.2023.101802 (2024).
14. Wahab, A., Ara, L., Shah, L. A., Naeem, H. & Hyeongmin Yoo. Synthesis of Bio-Based Hydroxyethyl Cellulose Superabsorbent Hydrogel for Successful Removal of Methylene Blue From Aqueous Medium. *J. Appl. Polym.* **143**, e70005. https://doi.org/10.1002/app.70005 (2026).
15. Zenebe, A., Din, K., Yimer, A. M., Kuzhunellil, S. & Demissie, H. Green synthesis of magnetic nanocomposite by Cordia africana leaf extract for the treatment of methylene blue contaminated water. *Chem. Eng. J. Adv.* **8**, 100193. https://doi.org/10.1016/j.ceja.2021.100193 (2021).
16. Melilli, G., Yao, J., Chiappone, A., Sangermano, M. & Hakkarainen, M. Photocurable all-lignocellulose derived hydrogel nanocomposites for adsorption of cationic contaminants. *Sustain. Mater. Technol.* **27**, e00243. https://doi.org/10.1016/j.susmat.2020.e00243 (2021).
17. Qian, H., Wang, J. & Yan, L. Synthesis of lignin-poly(N-methylaniline)-reduced graphene oxide hydrogel for organic dye and lead ions removal. *J. Bioresour Bioprod.* **5**, 204–210. https://doi.org/10.1016/j.jobab.2020.07.006 (2020).
18. Agorku, E. S., Kangmenna, A., Danu, B. Y., Ampong, F. K. & Voegborlo, R. B. Core-shell V_2O_5-gum ghatti grafted poly(acrylamide-co-methacrylic acid) adsorbent for the removal of methylene blue dye in water: kinetic, equilibrium and thermodynamic studies. *Next Sustain.* **5**, 100069. https://doi.org/10.1016/j.nxsust.2024.100069 (2025).
19. Gautam, S., Rasool, T. & Kumar, V. Hing gum-based hydrogel for effective adsorption of methylene blue and rhodamine B from wastewater: a comparative study. *Next Mater.* **8**, 100861. https://doi.org/10.1016/j.nxmate.2025.100861 (2025).
20. Al-Aidy, H. & Amdeha, E. Green adsorbents based on polyacrylic acid-acrylamide grafted starch hydrogels: the new approach for enhanced adsorption of malachite green dye from aqueous solution. *Int. J. Environ. Anal. Chem.* **101**, 2796–2816. https://doi.org/10.1080/03067319.2020.1711896 (2021).
21. Makhado, E. Preparation of carboxymethyl cellulose-based silica hydrogel nanocomposite for methylene blue and malachite green dyes adsorption from aqueous solution. *Surf. Interfaces*. **56**, 105699. https://doi.org/10.1016/j.surfin.2024.105699 (2025).
22. Seleka, W. M. & Makhado, E. Synthesis and characterization xanthan gum/acrylic acid/acrylamide modified with graphene oxide hydrogel nanocomposite for removal of methylene blue from aqueous solution. *Int. J. Biol. Macromol.* **305**, 141015. https://doi.org/10.1016/j.ijbiomac.2025.141015 (2025).
23. Lebkiri, I. et al. Swelling properties and basic dye adsorption studies of polyacrylamide hydrogel. *Desalin. Water Treat.* **233**, 361–376. https://doi.org/10.5004/dwt.2021.27530 (2021).
24. Hossain, S. et al. Jute cellulose nanocrystal/poly(N,N-dimethylacrylamide-co-3-methacryloxypropyltrimethoxysilane) hybrid hydrogels for removing methylene blue dye from aqueous solution. *J. Sci. Adv. Mater. Devices*. **6**, 254–263. https://doi.org/10.1016/j.jsamd.2021.02.005 (2021).
25. Moreno-Sader, K., García-Padilla, A., Realpe, A., Acevedo-Morantes, M. & Soares, J. B. P. Removal of heavy metal water pollutants (Co^{2+} and Ni^{2+}) using polyacrylamide/sodium montmorillonite (PAM/Na-MMT) nanocomposites. *ACS Omega*. **4**, 10834–10844. https://doi.org/10.1021/acsomega.9b00981 (2019).
26. Kumar, N., Mittal, H., Parashar, V., Ray, S. S. & Ngila, J. C. Efficient removal of rhodamine 6G dye from aqueous solution using nickel sulphide incorporated polyacrylamide grafted gum karaya bionanocomposite hydrogel. *RSC Adv.* **6**, 21929. https://doi.org/10.1039/C5RA24299A (2016).
27. Corona-Rivera, M. A., Ovando-Medina, V. M., Bernal-Jacome, L. A., Cervantes-Gonzalez, E. & Antonio-Carmona, I. D. Davila-Guzman. Remazol red dye removal using poly(acrylamide-co-acrylic acid) hydrogels and water absorbency studies. *Colloid Polym. Sci.* **295**, 227. https://doi.org/10.1007/s00396-016-3996-2 (2017).
28. Yang, X. et al. Polyacrylamide grafted cellulose as an eco-friendly flocculant: efficient removal of organic dye from aqueous solution. *Fibers Polym.* **18**, 1652. https://doi.org/10.1007/s12221-017-1216-4 (2017).
29. Zhao, W., Fan, Y., Wang, H. & Wang, Y. Coacervate of polyacrylamide and cationic gemini surfactant for the extraction of methyl orange from aqueous solution. *Langmuir* **33**, 6846–6856. https://doi.org/10.1021/acs.langmuir.7b01421 (2017).
30. Yan, C., Zhao, Y., Zhou, S. Y. & Chu, X. Z. Xing. Study on polyacrylamide/attapulgite clay composite adsorbent material. *J. Chem. Eng. Univ.* **24**, 274–279 (2010).
31. Yang, Y., Song, S. & Zhao, Z. Graphene oxide/polyacrylamide composite hydrogels as efficient cationic dye adsorbents. *Colloids Surf. Physicochem Eng. Asp*. **513**, 315. https://doi.org/10.1016/j.colsurfa.2016.10.060 (2016).

32. Ahmadi, S. et al. Hydrogel-based materials as antibacterial agents and super adsorbents for the remediation of emerging pollutants: a comprehensive review. *Emerg. Contam.* **10**, 100336. https://doi.org/10.1016/j.emcon.2024.100336 (2024).
33. Zdravković, A. et al. The removal of heavy metal ions from aqueous solutions by hydrogels based on N-isopropylacrylamide and acrylic acid. *Polym. Bull.* **75**, 4797–4821. https://doi.org/10.1007/s00289-018-2295-0 (2018).
34. Lin, Z. et al. Nitrogen-doped hydrochar prepared by biomass and nitrogen-containing wastewater for dye adsorption. *J. Environ. Manag.* **334**, 117503. https://doi.org/10.1016/j.jenvman.2023.117503 (2023).
35. Massrour, A., Peighambardoust, S. J., Foroughi, M., Foroutan, R. & Ramavandi, B. Crystal violet removal by sodium alginate-g-polyacrylamide/hydroxyapatite/Cu-Fe LDH nanocomposite. *Environ. Technol. Innov.* **38**, 104149. https://doi.org/10.1016/j.eti.2025.104149 (2025).
36. Zhang, C. et al. Self-assembled electrospun PVA/CMC/PEO composite fiber film material with enhanced dye adsorption performance for wastewater treatment. *Colloids Surf. Physicochem Eng. Asp.* **678**, 132461. https://doi.org/10.1016/j.colsurfa.2023.132461 (2023).
37. Morsi, R. E. & Elsalamony, R. A. Superabsorbent enhanced-catalytic core/shell nanocomposites hydrogels for efficient water decolorization. *New. J. Chem.* **40**, 2927. https://doi.org/10.1039/C5NJ02823J (2016).
38. Pourjavadi, A., Doulabi, M., Soleyman, R., Sharif, S. & Eghtesadi, S. A. Synthesis and characterization of a novel (salep phosphate)-based hydrogel as a carrier matrix for fertilizer release. *React. Funct. Polym.* **72**, 667–672. https://doi.org/10.1016/j.reactfunctpolym.2012.06.010 (2012).
39. Anil, I., Gunday, S. T., Bozkurt, A. & Alagha, O. Design of crosslinked hydrogels comprising poly(vinylphosphonic acid) and bis[2-(methacryloyloxy)ethyl] phosphate as an efficient adsorbent for wastewater dye removal. *Nanomaterials* **10**, 131. https://doi.org/10.3390/nano10010131 (2020).
40. Wijaya, R. et al. Surface modification of sodium alginate-polyvinyl alcohol hydrogel beads using low-pressure cold plasma and application for methylene blue removal from water. *Desalin. Water Treat.* **322**, 101152. https://doi.org/10.1016/j.dwt.2025.101152 (2025).
41. Ahmadijokani, F. et al. Arjmand. Waste organic dye removal using MOF-based electrospun nanofibers of high amine density. *Chem. Eng. J.* **466**, 143119. https://doi.org/10.1016/j.cej.2023.143119 (2023).
42. Marey, A., Adel, M., El Naggar, A. M. A., El-Zahhar, A. A. & Taha, M. H. Nickel-hydroxide-encapsulated polyacrylamide as a novel adsorptive composite for the capture of methylene blue from wastewater. *Dalton Trans.* **52**, 14194. https://doi.org/10.1039/D3DT02696E (2023).
43. Mittal, H., Al Alili, A. & Alhassan, S. M. High efficiency removal of methylene blue dye using jcarrageenan-poly(acrylamide-co-methacrylic acid)/AQSOA-Z05 zeolite hydrogel composites. *Cellulose* **27**, 8269–8285. https://doi.org/10.1007/s10570-020-03365-6 (2020).
44. Sawut, A., Wu, T., Simayi, R., Jiao, X. & Feng, Y. Preparation and Photocatalytic Performance of Sodium Alginate/Polyacrylamide/Polypyrrole-TiO_2 Nanocomposite Hydrogels. *Polymers* **15** (20), 4174. https://doi.org/10.3390/polym15204174 (2023).
45. Li, W. et al. Fabrication of novel starch-based composite hydrogel microspheres combining Diels–Alder reaction with spray drying for MB adsorption. *J. Environ. Chem. Eng.* **9**, 105929. https://doi.org/10.1016/j.jece.2021.105929 (2021).
46. Sehil, H., Badaoui, M. & Chougui, A. Preparation and characterization of a novel chemically crosslinked chitosan-g-polyacrylamide hydrogel as a promising adsorbent for the removal of methylene blue from aqueous solutions. *Polym. Sci. Ser. B.* **63**, 853–865. https://doi.org/10.1134/S1560090421060269 (2021).
47. Khatooni, H., Peighambardoust, S. J., Foroutan, R., Mohammadi, R. & Ramavandi, B. Adsorption of methylene blue using sodium carboxymethyl cellulose-g-poly(acrylamide-co-methacrylic acid)/Cloisite 30B nanocomposite hydrogel. *J. Polym. Environ.* **31**, 297–311. https://doi.org/10.1007/s10924-022-02623-x (2023).
48. Peighambardoust, S. J., Azari, M. M., Pakdel, P. M., Mohammadi, R. & Foroutan, R. Carboxymethyl cellulose grafted poly(acrylamide)/magnetic biochar as a novel nanocomposite hydrogel for efficient elimination of methylene blue. *Biomass Convers. Biorefin.* **15**, 15193–15209. https://doi.org/10.1007/s13399-024-06180-2 (2025).
49. Zhou, Q. et al. Tea polyphenol reinforced polyacrylamide hydrogel as a regenerative adsorbent for low-concentration methylene blue. *Colloids Surf. Physicochem Eng. Asp.* **698**, 134591. https://doi.org/10.1016/j.colsurfa.2024.134591 (2024).
50. Zhang, X. M., Zhang, Q., Gao, J. & Du, X. Y. Facile preparation of poly(AA-co-NaAMPS) hydrogels toward toxic dyes and heavy metals removal via frontal polymerization. *J. Polym. Sci.* **63**, 1352–1364. https://doi.org/10.1002/pol.20241124 (2025).
51. Huaman, M. A. L. et al. Removal of methylene blue dye from water with Fe_3O_4/poly(HEMA-co-AMPS) magnetic hydrogels. *Results Chem.* **7**, 101454. https://doi.org/10.1016/j.rechem.2024.101454 (2024).
52. Wu, Z., Wu, J., Huang, M., Liang, H. & Sun, B. Preparation of reusable hydrogel spheres based on sodium alginate/Fe_3O_4 modified with carboxymethyl huangshui polysaccharide and efficient adsorption performance for methylene blue. *Food Chem.* **438**, 138064. https://doi.org/10.1016/J.FOODCHEM.2023.138064 (2024).
53. Ilgin, P. et al. Adsorption of methylene blue from aqueous solution using poly(2-acrylamido-2-methyl-1-propanesulfonic acid-co-2-hydroxyethyl methacrylate) hydrogel crosslinked by activated carbon. *J. Macromol. Sci. A.* **60**, 135–149. https://doi.org/10.1080/10601325.2023.2165945 (2023).
54. Nakhjiri, M. T., Marandi, G. B. & Kurdtabar, M. Poly(AA-co-VPA) hydrogel cross-linked with N-maleyl chitosan as dye adsorbent: isotherms, kinetics and thermodynamic investigation. *Int. J. Biol. Macromol.* **117**, 152–166. https://doi.org/10.1016/j.ijbiomac.2018.05.140 (2018).
55. Nakhjiri, M. T., Marandi, G. B. & Kurdtabar, M. Effect of bis[2-(methacryloyloxy)ethyl] phosphate as a crosslinker on poly(AAm-co-AMPS)/Na-MMT hydrogel nanocomposite as potential adsorbent for dyes: kinetic, isotherm and thermodynamic study. *J. Polym. Res.* **25**, 244. https://doi.org/10.1007/s10965-018-1625-0 (2018).
56. Shukla, S., Pande, P. P., Chaurasiya, A., Chaudhary, A. & Kashaudhan, K. Copper oxide nanoparticle-doped hydrogel and its application for the removal of methylene blue dye from aqueous solutions. *Int. J. Environ. Anal. Chem.* **105** (20), 8645–8670. https://doi.org/10.1080/03067319.2025.2482174 (2025).
57. Kashaudhan, K. et al. Design of XGX-g-PAAHs@CuO nanocomposite for efficient removal of methylene blue from water. Separation Science and Technology, 60(11), 1350–1369 (2025). (2025). https://doi.org/10.1080/01496395.2025.2493281
58. Rai, U. et al. Facile Synthesis of Cobalt Oxide-Doped Hydrogel Nanocomposite for Efficient Methylene Blue Dye Removal. *Chem. Afr.* **8**, 2455–2473. https://doi.org/10.1007/s42250-025-01305-0 (2025).
59. Khatoon, A. et al. Cobalt oxide-embedded smart hydrogel nanocomposites for enhanced dye remediation from wastewater. *Sep. Sci. Technol.* **60** (15), 2041–2059. https://doi.org/10.1080/01496395.2025.2559293 (2025).
60. Kumar, R. et al. Synthesis and characterization of novel pectin-based copper oxide nanocomposite and its application for removal and photocatalytic degradation of methylene blue from aqueous solution. *Iran. Polym. J.* **34**, 65–81. https://doi.org/10.1007/s13726-024-01355-0 (2025).
61. Awode, A. U., Elaigwu, S. E., Oladipo, A. A. & Yilmaz, O. Gaz. Removal of Methylene Blue Dye from Aqueous Solution Using Trichlorovinylsilane Chitosan–g–polyacrylamide Hydrogel. *JOTCSA* **10** (4), 1009–1018. https://doi.org/10.18596/jotcsa.1292604 (2023).
62. Ansari, H., Oladipo, A. A. & Gazi, M. Alginate-based porous polyHIPE for removal of single and multi-dye mixtures: Competitive isotherm and molecular docking studies. *Int. J. Biol. Macromol.* **246**, 125736. https://doi.org/10.1016/j.ijbiomac.2023.125736 (2023).

63. Elessawy, N. A., Alhamzani, A. G. & Almahmoud, S. A. J. Hsiao. Evaluation, optimization study, and life cycle assessment of novel eco-friendly PVA-based nanocomposite hydrogel adsorbents for methylene blue and paracetamol removal. *Ecotoxicol. Environ. Saf.* **285**, 117123. https://doi.org/10.1016/j.ecoenv.2024.117123 (2024).
64. Meftah, S., Meftah, K., Addich, M. & Chahid, A. Comparative analysis of 13 types of adsorbent materials for water pollutant removal via a multi–criteria evaluation of performance cost circular economy green chemistry and durability. Meftah. *Discover Environ.* **4**, 257. https://doi.org/10.1007/s44274-026-00769-2 (2026).
65. Verma, Y. et al. Sharma. Green hydrogel as sustainable adsorbents: Bridging biopolymer & environmental remediation. *Adv. Industrial Eng. Polym. Res.* https://doi.org/10.1016/j.aiepr.2026.03.003 (2026).

Acknowledgements
This work was funded by the Deanship of Graduate Studies and Scientific Research at Jouf University under grant No. (DGSSR-2025-02-01452). The authors acknowledge support from the KIT-Publication Fund of the Karlsruhe Institute of Technology.

Author contributions
Author Contributions: A.A.N: Conceptualization, Investigation, Supervision, Funding acquisition, Writing-original draft, Writing-reviewing and editing. A.I.A.: Conceptualization, Investigation, Methodology, Software, Formal analysis, Writing-reviewing and editing. W.A.A.: Data curation, Formal analysis, Validation. I.M.A.: Software, Methodology, Visualization, Formal analysis. A.H.A.: Data curation, Software, Formal analysis. M.D.A.: Writing-original draft, Software, Formal analysis, Resources. A.G.M.: Methodology, Software, Formal analysis, Resources. M.A.A.: Conceptualization, Methodology, Software, Formal analysis, Resources. S.B. Funding acquisition, Supervision, Writing-original draft, Writing-reviewing and editing.

Funding
Open Access funding enabled and organized by Projekt DEAL. This work was funded by the Deanship of Graduate Studies and Scientific Research at Jouf University under grant No. (DGSSR-2025-02-01452). The authors acknowledge support from the KIT-Publication Fund of the Karlsruhe Institute of Technology.

Declarations

Competing interests
The authors declare no competing interests.

Declarations of generative AI use
During the preparation of this manuscript, generative AI tools were used solely to create Schemes 1 & 2 (and not for writing the manuscript). The authors accept full responsibility for the accuracy and integrity of the manuscript.

Additional information
Supplementary Information The online version contains supplementary material available at https://doi.org/10.1038/s41598-026-64487-8.

Correspondence and requests for materials should be addressed to A.A.N. or S.B.

Reprints and permissions information is available at www.nature.com/reprints.

Publisher's note Springer Nature remains neutral with regard to jurisdictional claims in published maps and institutional affiliations.

Open Access This article is licensed under a Creative Commons Attribution 4.0 International License, which permits use, sharing, adaptation, distribution and reproduction in any medium or format, as long as you give appropriate credit to the original author(s) and the source, provide a link to the Creative Commons licence, and indicate if changes were made. The images or other third party material in this article are included in the article's Creative Commons licence, unless indicated otherwise in a credit line to the material. If material is not included in the article's Creative Commons licence and your intended use is not permitted by statutory regulation or exceeds the permitted use, you will need to obtain permission directly from the copyright holder. To view a copy of this licence, visit http://creativecommons.org/licenses/by/4.0/.

© The Author(s) 2026